Climate Dynamics (2019) 52:6989–7011
https://doi.org/10.1007/s00382-018-4561-0

Impact of multiyear La Niña events on the South and East Asian summer monsoon rainfall in observations and CMIP5 models

S. N. Raj Deepak[1,2] · Jasti S. Chowdary[1] · A. Ramu Dandi[1] · G. Srinivas[1,3] · Anant Parekh[1] · C. Gnanaseelan[1] · R. K. Yadav[1]

Received: 27 June 2018 / Accepted: 27 November 2018 / Published online: 1 December 2018

Abstract

Impact of multi-year La Niña events on South and East Asian summer monsoon rainfall are examined in the observations and Coupled Model Intercomparison Project Phase 5 (CMIP5) models. The analysis is carried out for the successive two summers, referred to as the first and second years during the period of 1948–2016. Composite analysis suggests that La Niña related sea surface temperature cooling is slightly high in the central and eastern equatorial Pacific during the first year summer. This anomalous cooling associated with La Niña is slightly shifted towards south and south-central Pacific Ocean during the second year. An Atlantic Niño like pattern is evident in the first year unlike the second year. Negative rainfall anomalies are apparent over most of the south Asian region except Bangladesh and Sundarbans, during the first year. Moisture convergence corroborated by low-level circulation to the north of Bangladesh and central India supports the positive rainfall anomalies in the first year. A weak circulation and negative vertically integrated moisture (VIM) anomalies in the rest of the subcontinent are consistent with the negative rainfall anomalies. In addition to these changes, the Atlantic Niño has also been found to be influencing the South Asian rainfall, remotely, during the first year. In the case of the second year, positive rainfall anomalies over the south Asian monsoon region is noted. An anomalous low-level cyclonic circulation over the central Bay of Bengal enhanced the moisture transport into the Indian subcontinent, causing positive rainfall anomalies. Moreover, an anomalous upper level divergence extends from the southeast Indian Ocean, towards the Indian subcontinent, due to La Niña's response in the second year, which is found to be weak in the first year. This clearly suggests that the enhanced rainfall over the South Asian region is influenced remotely by La Niña forcing as well as local circulation changes during both the years. The East Asian monsoon region reported a tri-pole like structure in the rainfall anomalies, with positive values over southern and central China and negative over parts of Myanmar, Thailand and Cambodia regions and north-east China—North Korea during the first year and vice-versa in the second year. A positive–negative–positive structure in the VIM anomalies is seen in the East Asian region and it supports similar rainfall anomalies during the second year. We have further examined the ability of CMIP5 models in representing multiyear La Niña teleconnections to the south and East Asian summer monsoons. Some models are able to reproduce the South Asian rainfall and circulation anomalies well in the second year, but failed to do so, in the first. The factors responsible for weak teleconnections in the models are discussed in detail.

Keywords Asian summer monsoon rainfall · Multiyear La Niña · Precipitation · Sea surface temperature · Atmospheric teleconnections

1 Introduction

El Niño Southern Oscillation (ENSO) phenomenon is mainly responsible for the interannual fluctuations in the tropical Pacific Ocean sea surface temperature (SST). These year to year SST variations have impacts on the weather and climate over several parts of the globe (e.g., Angell 1981; Keshavamurthy 1982; Gill and Rasmusson 1983; Philander 1983; Rasmusson 1985; Webster and Yang 1992;

✉ Jasti S. Chowdary
jasti@tropmet.res.in

[1] Indian Institute of Tropical Meteorology, Pune 411008, India

[2] Savitribai Phule Pune University, Pune 411007, India

[3] Indian National Centre for Ocean Information Services, Hyderabad 500090, India

Gordon and Fine 1996; Kripalani and Kulkarni 1997; Trenberth and Hoar 1997; Alexander et al. 2002; Andrews et al. 2004). Many studies suggest that the cold SST anomalies over east equatorial Pacific Ocean indicates above normal monsoon rainfall over the south Asian region (e.g., Sikka 1980; Pant and Parthasarathy 1981; Bhalme et al. 1983; Van Loon and Shea 1985; Webster and Yang 1992; Kumar et al. 1995, 1999; Kripalani and Kulkarni 1997; Yadav 2009a). On the contrary, there have been years where droughts have occurred during La Niña events (e.g., Kumar 1995). The East Asian summer monsoon consists of two subsets: the East Asian summer monsoon (consisting of the Meiyu-Baiu regions) and the western north Pacific summer monsoon. These two monsoons by themselves, follow an out-of-phase condition. Studies have described that the western north Pacific summer monsoon tends to be stronger following the matured phase in La Niña, while the East Asian summer monsoon is below normal (e.g., Webster et al. 1998; Boahua and Ronghui 1999; Li and Mu 2000; Wang et al. 2001, 2003; Huang et al. 2007 etc.). Previous studies have noted that the impacts of El Niño and La Niña are not symmetric in many aspects (e.g., Hoerling et al. 1997; Wu et al. 2010; Hu et al. 2014). Several studies have also reported the asymmetry in the temporal evolution between El Niño and La Niña (e.g., Kessler 2002; Kug et al. 2005; Ohba and Udea 2009; Okumura and Deser 2010; Okumura et al. 2011; Chen et al. 2016; Hu et al. 2017). In general, El Niño events tend to decay rapidly by the summer, following the peak phase, but La Niña events persist through the year and re-intensify during the subsequent winter, thus occurring as multiple-year events (2 year) (e.g., Okumura and Deser 2010; Hu et al. 2014). Thus, majority of the La Niña events decay slowly and take several years to return to near-neutral conditions (e.g., Kessler 2002).

Hu et al. (2014) suggested that a strong La Niña causes the subsurface ocean to remain cold. This interrupts the recharge phase in the absence of downwelling equatorial Kelvin waves after the first year. Weaker wind response to negative SST anomalies cause a weaker thermocline recharge and an ineffective termination of the La Niña events (e.g., Frauen and Dommenget 2010; Okumura et al. 2011; Ohba and Ueda 2009; Choi et al. 2013; DiNezio and Deser 2014). This supports the persistent cooling over the east equatorial Pacific. DiNezio and Deser (2014) suggested from coupled model sensitivity experiments that the nonlinearity in the delayed thermocline feedback controls the duration of the La Niña events. Some studies indicated that the incursion of off-equatorial subsurface cold water triggers the double dip in La Niña events (e.g., Zheng et al. 2015; Feng et al. 2015). Luo et al. (2017) reported that the intensification of easterly winds in the central equatorial Pacific, largely induced by warm SST anomalies in the Atlantic and Indian Oceans mainly contributed to the occurrence of the 2 year La Niña 2010–2012. The manifestation of an anomalous Walker circulation during boreal summer associated with the Atlantic Niño helps in the development of full La Niña conditions by the following winter (e.g., Rodriguez-Fonseca et al. 2009; Polo et al. 2014; Kucharski et al. 2016). On the other hand, DiNezio et al. (2017a) suggested that the magnitude and persistence of subsurface temperature anomalies were useful for the prediction of La Niña duration. Further, DiNezio et al. (2017b) predicted 2 year La Niña events with a 60% probability based on a climate model and an 80% probability based on an empirical model.

Effects of multi-year La Niña events, which extended for 2 years, on the tropical and subtropical climate have been carried out by some researchers. For example, La Niña episode during 2010–2012 decreased the global surface temperature, increased precipitation, terrestrial water storage in some regions particularly over Australia (e.g., Luo et al. 2017). Boening et al. (2012) reported that this long-lived La Niña caused global mean sea level drop by 5 mm, opposing the long-term rise in response to global warming. Okumura et al. (2017) examined the atmospheric teleconnections during multiyear La Niña events and its influence on the United States' (U.S.) precipitation anomalies. They found that these La Niña events exert significant impacts on drought like conditions over the southern U.S. during boreal winter season. Singh et al. (2013) noted that long-lived La Niña events cause anomalous SST cooling over the southwest tropical Indian Ocean through atmospheric teleconnections and reduces the local convection. This contributes to the reduced rainfall over the northern parts of Madagascar. Further, Barlow et al. (2002) suggested that the atmospheric teleconnections associated with these long-lived La Niña events have strong impact on the winter rainfall anomalies over central Asia. Most of the works carried out were related to winter precipitations over different regions during multi-year La Niña events. Previous studies have not addressed the impact of teleconnections of multiyear La Niña events on the South and East Asian summer monsoon rainfall variations. It is not clear how these multiyear La Niña events affect the evolution of atmospheric teleconnections to South and East Asia. This issue is addressed in the present study. Section 2 presents the details of data and models used in this study. In Sect. 3, evolution of SST anomalies and associated rainfall patterns are discussed. Atmospheric teleconnections associated with multiyear La Niña events during summer are described in Sect. 4. Section 5 examines the ability of CMIP5 models in representing the teleconnections. Summary is provided in Sect. 6.

2 Data, methodology and modes used

We have used the National Centers for Environmental Prediction/National Center for Atmospheric Research (NCEP/NCAR) sea level pressure (SLP), zonal, meridional and

vertical (omega) winds, air temperature, specific humidity and geopotential heights (GPH) (Kalnay et al. 1996) for the period of 1948–2016 for all levels. SST data is obtained from Hadley Center Sea Ice and SST (HadISST) (Rayner et al. 2003) data. High resolution (0.5° × 0.5°) global land rainfall from Climate Research Unit (CRU) data (Harris et al. 2014) and Indian land rainfall from India Meteorological Department (IMD) (Pai et al. 2015; Rajeevan et al. 2006) have been also used. Monthly anomalies are derived relative to the climatological mean of the study period 1948–2016 and detrended in order to remove the trend. The Niño-3.4 index is calculated by averaging SST anomalies over the eastern Pacific from 5°S to 5°N, 170° to 120°W.

The World Climate Research Programme (WCRP) Coupled Model Intercomparison Project Phase 5 (CMIP5) Data (Taylor et al. 2012) are used in this study. The details of 38 models are mentioned in Table 1. The table also mentions the number of continuous La Niña events in each model. Each of these models was run under the label "historical runs" and only the first ensemble member (r1i1p1) has been considered. The monthly data of the years 1901–2005 for the twentieth century is utilized. The SST data is of the resolution 1° × 1° for all the models considered and the atmospheric dataset is of the resolution 2° × 2°. Composites analysis is carried out in this study and two tailed Student's *t* test have been performed to extract the significant signals. Further we have computed the velocity potential, vertically integrated moisture transport (VIMT; Godfred-Spenning and Reason 2002) and Wave Activity Flux (Takaya and Nakumara 2001).

We define 2-year La Niña (multiyear) events as those with a Niño-3.4 SST index less than −0.75 standard deviations for two consecutive winters (December–January–February; DJF) seasons and less than −0.5 in the next summers (June–July–August; JJA).

3 Evolution of multiyear La Niña SST anomalies and associated rainfall patterns

Figure 1 depicts the evolution of SST anomalies from years 1948 to 2016 (time-longitude plots) in the equatorial Pacific region averaged from 5°S to 5°N. A total of 11 La Niña developing years 1949, 1954, 1961, 1967, 1970, 1973, 1983, 1988, 1995, 1998, and 2010 are noticed during the period of 1948–2016 which is consistent with earlier studies (e.g., Okumura et al. 2011; Hu et al. 2014). Significant negative SST anomalies over the central to east equatorial Pacific region for 2 consecutive years are noted. Time series of DJF Niño-3.4 index normalized SST anomalies also confirm the same (figure not shown). Our interest is to examine the summer teleconnections after the peak phase of La Niña, of consecutive 2 year La Niña DJF peaks. Thus, this study considered only 2 year La Niña events and the analysis are carried out for the following summers after a peak phase of La Niña, referred to as the first and second years. Note that the La Niña events are considered only if cold SST conditions prevailed in the east and central equatorial Pacific for the summer after the second La Niña peak (hereafter multiyear La Niña events). Developing La Niña year summers (referred to as initial year) are not taken into account, because, cold SST anomalies over the equatorial Pacific could not develop completely in many cases and their impacts varied from case to case. We have identified four multiyear La Niña events during the study period. It is found that only 1954, 1973, 1983 and 1998 have satisfied the above criteria and following two summer years are considered for analysis. Thus, the main focus is on the first and second summer monsoon years after the initial DJF peak, which are 1955–1956, 1974–1975, 1984–1985 and 1999–2000. During these years prolonged negative SST anomalies over the ENSO region is apparent without any interruption (Fig. 1). This is further evident in the temporal evolution of normalized Niño-3.4 SST anomalies for individual years and their composite during all seasons of multiyear La Niña events (Fig. 2a).

Composite analysis suggests that the anomalous cooling corresponding to La Niña is slightly greater in the central and eastern equatorial Pacific during the first year summer (Fig. 2b). In the second year, this anomalous cooling is slightly shifted towards the south and south-central Pacific Ocean (Fig. 2c). On the other hand, the southern TIO is cooler in the first year, while the northern parts displayed negative SST anomalies during the second year (Fig. 2d). Parts of the South China Sea are significantly cooler during both the years. Added to this, the southeast equatorial Atlantic Ocean is significantly warm during the first year, representing Atlantic Niño like pattern, unlike in the second year, which is also apparent in the difference between first and second years (Fig. 2d). The Atlantic Niño which peaks during the boreal summer, is preceded by equatorial westerly wind perturbations (e.g., Zebiak 1993; Keenlyside and Latif 2007; Deppenmeier et al. 2016). However, compared with that of the Pacific, the Bjerknes coupling strength is weaker by the order of 50% (e.g., Lübbecke and Mcphaden 2013). This clearly suggests that the weak air-sea coupling in the Atlantic (as compared to Pacific) is the possible reason for the inability to maintain the Atlantic Niño in the second year. It is noted that, three out of four events used for composite analysis displayed Atlantic Niño pattern and 1 year showed very weak warm anomalies (figure not shown). In the first and second years, surface (1000 hPa) winds show significant easterly anomalies in the central and western equatorial Pacific region which is consistent with the SST cooling and corresponds to the La Niña phase (Fig. 2b, c). But, the predominant feature of the South Asian monsoon, the cross

Table 1 List of CMIP5 models considered, their modelling groups and the number of continuous La Niña events in each model

Model	Institution	No. of continuous La Niña events
ACCESS1-0	Commonwealth Scientific and Industrial Research Organization, Australia	2
ACCESS1-3	**Commonwealth Scientific and Industrial Research Organization, Australia**	**7**
BCC-CS1-1	Beijing Climate Centre, China Meteorological Administration, China	0
BCC-CSM1-1-m	Beijing Climate Centre, China Meteorological Administration, China	0
CanEsm2	Canadian Centre for Climate Modelling and Analysis, Canada	0
CCSM4	**National Centre for Atmospheric Research, USA**	**5**
CESM-1-BGC	National Centre for Atmospheric Research, USA	3
CESM1-FASTCHEM	National Centre for Atmospheric Research, USA	1
CESM-WACM	National Centre for Atmospheric Research, USA	2
CMCC-CM	**Centro Euro-Mediterraneo per I Cambiamenti Climatici, Italy**	**4**
CRNM-CM5-2	Centre National de Recherches Meteorologiques, France	0
CSIRO-MK-3-6-0	Commonwealth Scientific and Industrial Research Organization, Australia	1
FGOALS	State Key Laboratory of Numerical Modelling for Atmospheric Sciences and Geophysical Fluid Dynamics (LASG), Institute of Atmospheric Physics, China	0
FIO ESM	First Institute of Oceanography, China	1
GFDL-CM2P1	Geophysical Fluid Dynamics Laboratory, USA	2
GFDL-CM3	Geophysical Fluid Dynamics Laboratory, USA	0
GFDL-ESM2G	Geophysical Fluid Dynamics Laboratory, USA	2
GFDL-ESM2M	**Geophysical Fluid Dynamics Laboratory, USA**	**5**
GISS-E2-H	NASA Goddard Institute for Space Studies, USA	2
GISS-E2-H-CC	NASA Goddard Institute for Space Studies, USA	1
GISS-E2-R	NASA Goddard Institute for Space Studies, USA	2
GISS-E2-R-CC	NASA Goddard Institute for Space Studies, USA	0
HadGEM2-A0	National Institute of Meteorological Research/Korea Meteorological Administration, South Korea	1
HadGem2-CC	Met office Hadley Centre, UK	1
HadGem2-ES	Met office Hadley Centre, UK	1
INM-CM4	Institute for Numerical Mathematics, Russia	2
IPSL-CM5A-LR	**Institut Pierre-Simon Laplace, France**	**4**
IPSL-CM5A-MR	Institut Pierre-Simon Laplace, France	3
IPSL-CM5B-LR	Institut Pierre-Simon Laplace, France	2
MIROC5	**Atmosphere and Ocean Research Institute (The University of Tokyo), National Institute for Environmental Studies, and Japan Agency for Marine-Earth Science and Technology, Japan**	**11**
MIROC-ESM-CHEM	**Atmosphere and Ocean Research Institute (The University of Tokyo), National Institute for Environmental Studies, and Japan Agency for Marine-Earth Science and Technology, Japan**	**4**
MPI-ESM-LR	Max Planck Institute for Meteorology (MPI-M), Germany	3
MPI-ESM-MR	**Max Planck Institute for Meteorology (MPI-M), Germany**	**4**
MPI-ESM-P	**Max Planck Institute for Meteorology (MPI-M), Germany**	**4**
MRI-CGCM3	Meteorological Research Institute, Japan	2
MRI-ESM1	Meteorological Research Institute, Japan	3
NorESM1-M	Norwegian Climate Centre, Norway	1
NorESM1-ME	Norwegian Climate Centre, Norway	2

Models in bold are those which have greater than or equal to 4 events and are considered for composite analysis

equatorial flow, is insignificant. On the other hand, the cross equatorial flow in the Indian Ocean is visible and an anomalous cyclonic circulation is present in the Bay of Bengal during the second year (Fig. 2c). Difference between the first and second year surface winds shows divergent flow over the Indian subcontinent and eastern Bay of Bengal supports the modulation in rainfall patterns (Fig. 2d). A large difference in the low level circulations between western north Pacific

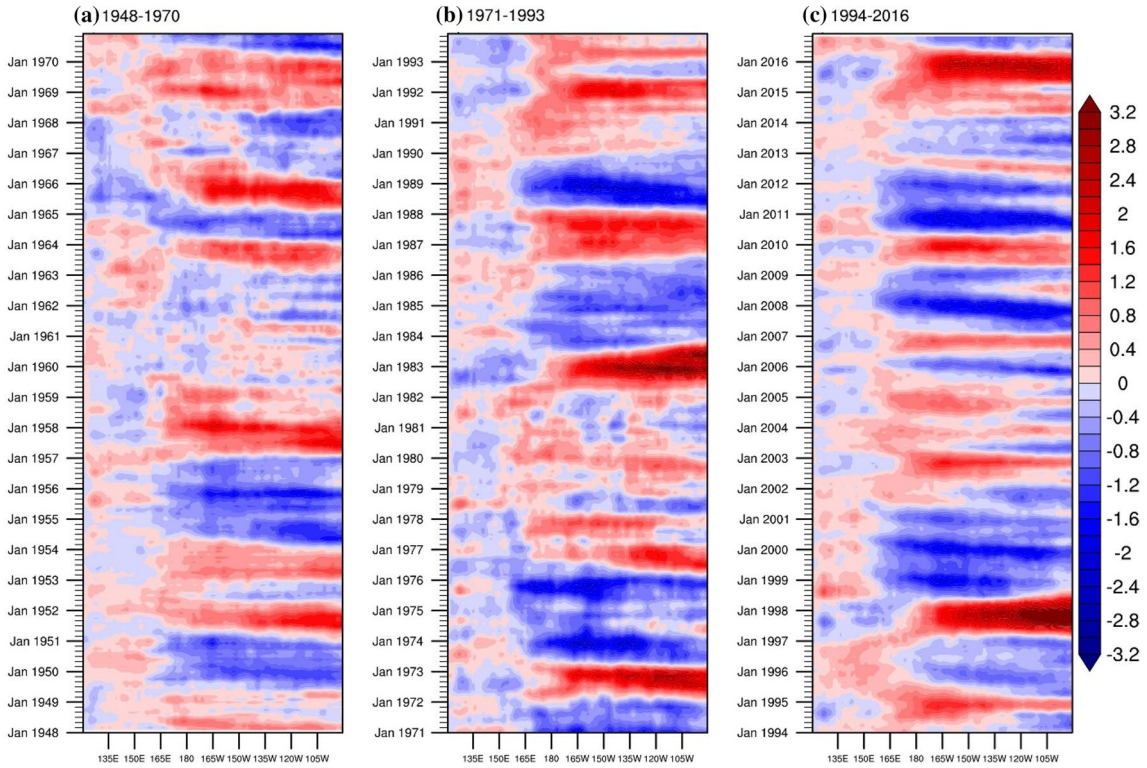

Fig. 1 Hovmoller plot depicting the evolution of SST anomalies (°C) over equatorial Pacific region, averaged for 5°N–5°S for the years 1948–2016. **a** 1948–1970; **b** 1971–1993; **c** 1994–2016

and East Asia is apparent between both the years. These circulations are known to have strong impacts on the local rainfall over the East Asian region.

To examine the multiyear La Niña-summer teleconnections, we have plotted composite of precipitation anomalies over the south and East Asia regions as illustrated Fig. 3. In the first year, the south Asian region is mostly covered with negative anomalies, but, the Sundarbans, Bangladesh and surrounding regions and parts of central India receive heavy rainfall. This follows the dipole pattern in rainfall as showed by Yadav et al. (2018), where positive and negative anomalies are seen over the northeast, northwest and central Indian regions, respectively. This feature attributes to the influence of Atlantic Niño. A tri-pole like structure in rainfall is seen in the East Asian region with positive anomalies over southern and central China and negative over north-east China–North Korean and parts of Myanmar, Thailand and Cambodia regions. The seasonal rainfall of second year shows a dramatic shift in the anomalous rainfall pattern. Heavy positive rainfall anomalies over the south Asian countries is noticed unlike the first year (Fig. 3b). The Sundarbans receive lesser rainfall. Nearly a mirror image of the first year tri-pole rainfall anomaly structure over the East Asian region is seen during the second year. However, Japan received lesser rainfall in both the years, more so in the second year. It is important to note that difference of first and second year rainfall is significant, both over the south and south-east Asian regions (Fig. 3c). To check the integrity of CRU rainfall data, fine resolution, homogeneous IMD rainfall data ($0.25° \times 0.25°$) is used in this study. Similar to the CRU data, the IMD rainfall also displayed positive rainfall anomalies in the regions surrounding Bangladesh, central and interior peninsular India, while rest of the country displayed negative rainfall anomalies in the first year (Fig. 3d). In the second year, India as a whole experienced positive rainfall anomaly except for a few places along the west coast and north-east region (Fig. 3e), this pattern is similar to that, when the contemptuous co-variability of Atlantic Niño is removed from El-Niño and Indian rainfall (e.g. Yadav et al. 2018). There is a shift in positive rainfall anomalies from the Eastern Himalayan foothills in the first year to the central Himalayan foothills in the second year. The monsoon core (monsoon trough), central and eastern peninsular regions receive high rainfall in the second year (Fig. 3f), as compared to the first year.

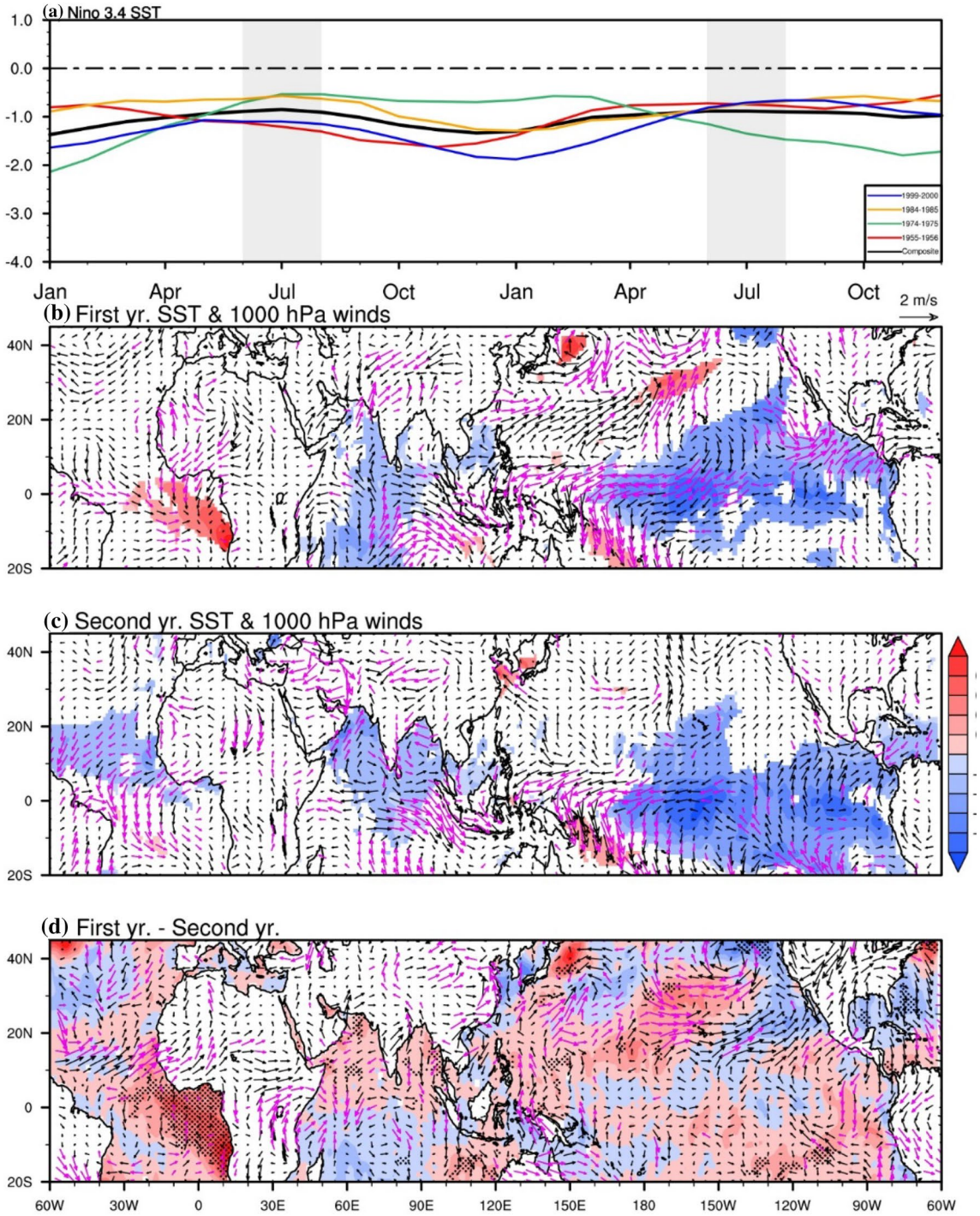

Fig. 2 **a** Time series Niño 3.4 (normalized) SST anomaly associated with multi-year La Niña events (boxes depict the summers considered in the present study). Composite of JJA SST anomalies at 85% confidence level (shaded; °C) overlaid with seasonal 1000 hPa wind anomalies (black vectors; m/s) at 85% confidence level (magenta vectors; m/s), with scaling as mentioned, **b** for the 1st year and **c** same as in **b**, but for the 2nd year. **d** Same as in **b** and **c**, but for differences (shaded; °C) in 1st year and 2nd year at 85% confidence level (black dots)

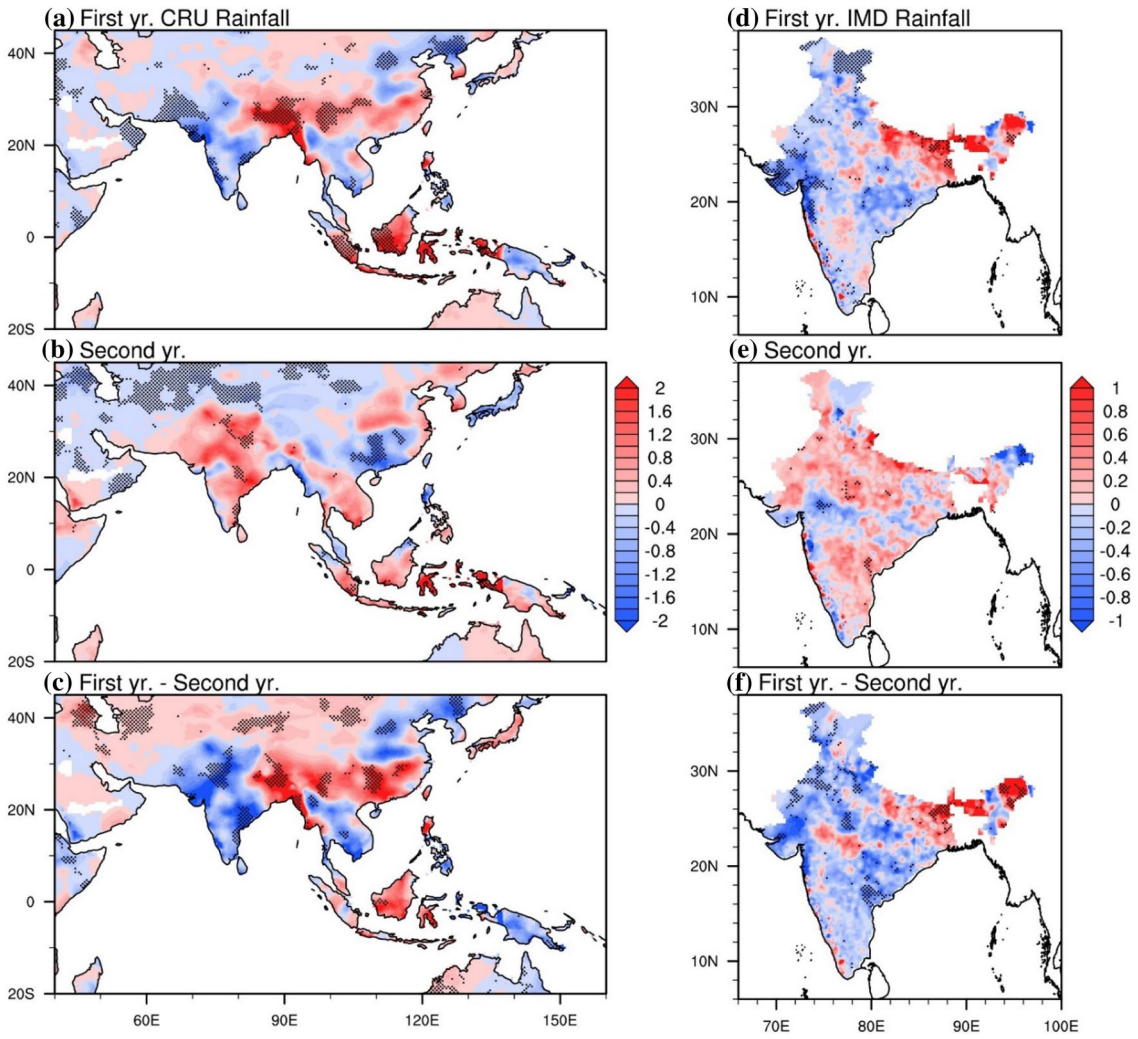

Fig. 3 Composite of JJA normalized CRU land precipitation anomalies for South and East-Asian regions (shaded), with 85% confidence anomalies (dots). **a** For 1st year, **b** same as in **a**, but for the 2nd year, **d** and **e** are same as in **a** and **b**, but for IMD rainfall. **c** Same as in **a** and **b**, but for difference in 1st year and 2nd year in CRU precipitation, **f** is same as in **c**, but for IMD rainfall

4 Observed atmospheric teleconnections associated with multiyear La Niña events during summer

4.1 Local atmospheric circulation changes

Figure 4 a, b depicts the seasonal SLP anomalies and significant points at 80% confidence level for the Indo-Pacific region, along with seasonal 850 hPa wind anomalies. In the first year, the significant negative SLP anomalies lie along the foothills of Himalayas in the Indian region. This means that the seasonally averaged position of the monsoon trough lies in that region, which is placed northward to its normal position. The Indian subcontinent, north-east China and Korean Peninsula and Thailand–Cambodia regions displayed weak SLP anomalies which are consistent with the negative rainfall anomalies in these regions. Strong convergence of wind is also apparent around 25°N over the Sundarbans region. The corresponding cross-equatorial flow is weak in the Indian Ocean and a weak cyclonic circulation is seen in the northern parts of India, consistent with the negative SLP anomalies (Fig. 4a). Strong trade winds from the central Pacific and the westerly flow across the southern Bay of Bengal converge over the Maritime Continent and it is apparent in the first year. An anomalous cyclonic circulation along with significant negative SLP anomalies are present over the western north Pacific Ocean. This inputs moisture to the southern Korean Peninsular region and south-east China. A weak anomalous cyclonic circulation is also present over central-south China. These two cyclonic circulations help to maintain the positive rainfall over these regions. Low-level winds are divergent over the central and south China, which

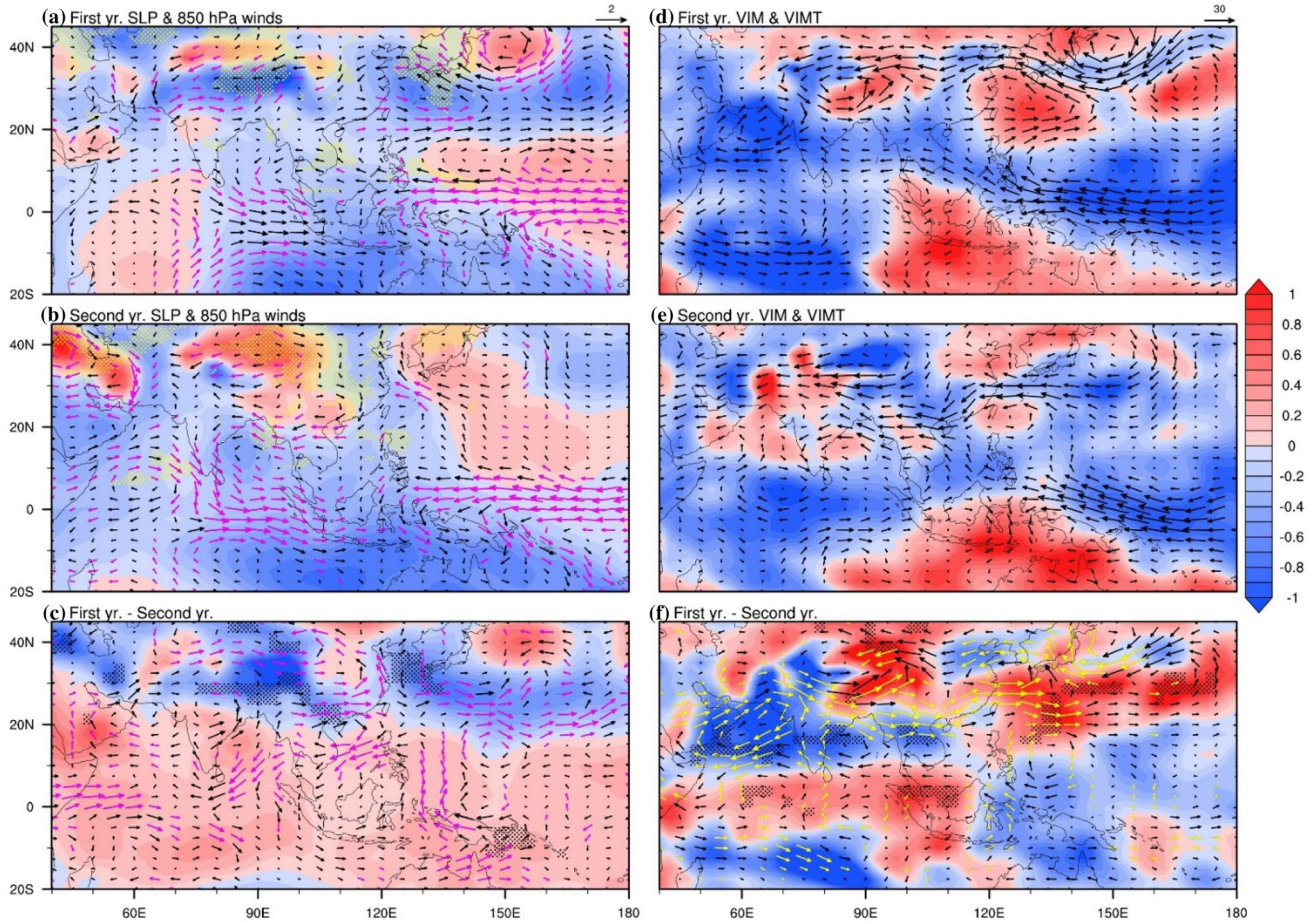

Fig. 4 **a** and **b** Composite of JJA SLP anomalies (shaded; hPa) overlaid with SLP anomalies at 80% confidence level (yellow dots), 850 hPa wind anomalies (black vectors; m/s) at 80% confidence level (magenta vectors; m/s). **d** and **e** Composite of JJA VIM anomalies (shaded; kg/m^2) overlaid with seasonal VIMT anomaly vectors (kg/m/s), with scaling as mentioned. **a** and **c** For the 1st year, **b** and **d** for the 2nd year. **c** Differences in 1st year and 2nd year for SLP and 850 hPa winds (black vectors) at 80% confidence level (magenta vectors). **f** Difference in 1st year and 2nd year for VIM (shaded) at 80% confidence level (black dots) and VIMT (black vectors) at 80% confidence level (yellow vectors)

are associated with cyclonic circulation south of 10°N and anticyclonic circulation north of 10°N. This circulation pattern supports the rainfall distribution over the parts of East Asian region (Figs. 3a, 4a). These circulation patterns are better visualized from rotational wind and stream function (figure not shown).

In the second year the significant negative SLP anomalies are mostly absent over India. The cross-equatorial flow and anomalous cyclonic circulation over central Bay of Bengal and South China Sea are present (Fig. 4b). The north periphery of this cyclonic circulation drags moisture from the South China Sea into Indo-China region. The 850 hPa wind anomalies and the rotational winds further suggests that, in the second year, the anomalous cyclonic circulation is elongated and positioned over the whole of Bay of Bengal. This supports the increased rainfall over the central and peninsular regions of the Indian subcontinent. Since the core of this cyclonic circulation extends to the Indo-China peninsular region, positive rainfall anomalies are seen. This is also supported by the negative SLP anomalies present in the South Asian monsoon region (Figs. 3b, 4b). The center of the anomalous anticyclonic circulation is seen over Japan, and thus the reduced rainfall activity over that region. The elongated cyclonic circulation off coast north-east China and the anticyclonic circulation over northwest Pacific together guide the moist winds toward the Yellow Sea region. This, along with the negative SLP anomalies over that region help in maintaining the positive rainfall anomalies. The presence of a weak anticyclonic circulation over south-east China and the associated positive SLP anomalies result in the negative rainfall anomalies. Difference in the low level circulation and SLP between the first and second years (Fig. 4c) is consistent with the difference in rainfall (Fig. 3c), and

with divergence (convergence) over the Indian subcontinent (central-China region).

To understand the factors which are responsible for rainfall patterns over the south and east-Asian region associated with multiyear La Niña events, VIM and VIMT have been analyzed. Figure 4d depicts the seasonal VIM and VIMT anomalies over the Indo-western Pacific region for the first years. It is noted from the VIMT, that the moisture converges to the north of Bangladesh and central India, which is consistent with the positive rainfall anomalies, while rest of the subcontinent shows negative VIM anomalies which are in line with negative rainfall anomalies. Anomalous negative VIM over Cambodia and Thailand supports negative rainfall anomalies. This can be directly related to the accumulation of moisture from both Pacific and Indian Ocean during La Niña years. In the second year, almost the whole Indian subcontinent displayed positive VIM anomalies (Fig. 4e). Presence of the cyclonic circulation over central Bay of Bengal helps transporting moisture into the Indian peninsula as well as towards the monsoon trough region and the entire subcontinent received increased rainfall in contrast to the first year. Moisture input from Yellow Sea to parts of northeast China and North and South Korea is visible and thus the increased rainfall in those regions. Low moisture winds from northeast China to central and southern parts somewhat explains negative rainfall anomalies in the latter region. On the other hand, moisture transport and positive VIM anomalies from South China Sea to land region supports positive rainfall anomalies over Cambodia and Thailand regions (Figs. 3b, 4e). Like the previous year, convergence of moisture laden winds from both the oceans, over the Maritime Continent, increases the rainfall anomalies over that region. Significant differences in VIM and VIMT between the first and second years are in line with rainfall changes (Figs. 3c, 4f).

4.2 Large-scale circulation changes associated with La Niña and Atlantic Niño

It is clear from the earlier discussion that changes in local circulation patterns and moisture transport largely influence the summer rainfall distribution over south and East Asia in both the years. But, is important to explore how La Niña forcing from central and eastern equatorial Pacific alter the circulation and rainfall over the Indo-Western Pacific in both the years (e.g., Kumar et al. 1995; Yadav 2009b). Figure 5a shows the seasonal 200 hPa velocity potential anomalies and divergent components of winds for the first year. Anomalous upper level convergence associated with La Niña related SST cooling is apparent over the central equatorial Pacific during the first year. The center of this convergence zone is placed slightly westward in second year as compared to first year, which is co-located with positive velocity potential anomalies (Fig. 5b). This shift in upper level convergence zone is further evident in the difference between the first and second years (Fig. 5c). Thus, the atmospheric response to SST anomaly patterns in first and second year is slightly different. In response to La Niña, anomalous upper level divergence is extended from southeast Indian Ocean to the Indian subcontinent in the second year. Such strong anomalies over south Asian region are not seen in the first year. This clearly suggests that enhanced rainfall over the Indian subcontinent in the second year is influenced remotely by La Niña forcing as well as local circulation changes. In the first year strong upper level divergence is seen over the equatorial Atlantic in response to the warm SST anomalies which corresponds to Atlantic Niño (Lübbecke and McPhaden 2013). Earlier studies suggested that the Atlantic Niño could influence summer monsoon rainfall over India apart from ENSO (e.g., Yadav et al. 2018; Pottapinjara et al. 2014; Kucharski et al. 2009; Yadav 2009a). Figure 5d, e shows the seasonal zonal circulation over the Indo-Pacific region averaged over the latitudinal belt of 5°N and 20°N. In the first year the ascending limb is contracted at 95°E, while it is zonally stretched from 85°E to 120°E and stronger in the second year. This difference in circulation supports the rainfall patterns in the first and second years (Fig. 5f). The descending limbs are situated to the east of the South China Sea and over the central Pacific regions in response to La Niña related SST anomalies. Ascending branch in response to Atlantic Niño is evident in the first year, whereas it is absent in the second year. The differences in the over-turning circulation shows enhanced vertical motion over the south Asian region (in the second year) and the Atlantic Niño region (in the first year). This supports the differences in rainfall patterns over the Indo-Western Pacific region (Fig. 5f).

In response to the equatorial SST cooling associated with La Niña, a pair of upper level cyclonic circulation systems are apparent as part of Matsuno–Gill pattern (Matsuno 1966; Gill 1980) during both the years (Fig. 6). Upper tropospheric cyclonic circulation anomalies are induced due to the diabatic cooling. They are formed to both sides of the equator and are caused by the suppressed precipitation over the equatorial Pacific. It is noted that centers of cyclonic circulations are situated slightly away from the equator in the first year and closer in the second year (Fig. 6a, b). These cyclonic circulation anomalies emanate a Rossby wave train into the northern hemisphere. In the first year, the wave train shows the Pacific-North American (PNA) pattern with meridional negative, positive and negative GPH anomalies arching from the subtropical north Pacific to the U.S. In case of the second year, the wave train stretches poleward as compared to the first year, which is also apparent in the difference (Fig. 6c). Recently Okumura et al. (2017) described the difference in PNA pattern between first and second year (preceding) winter seasons (during the peak phase of La Niña). They found that the precipitation over parts of the U.S. decreased not

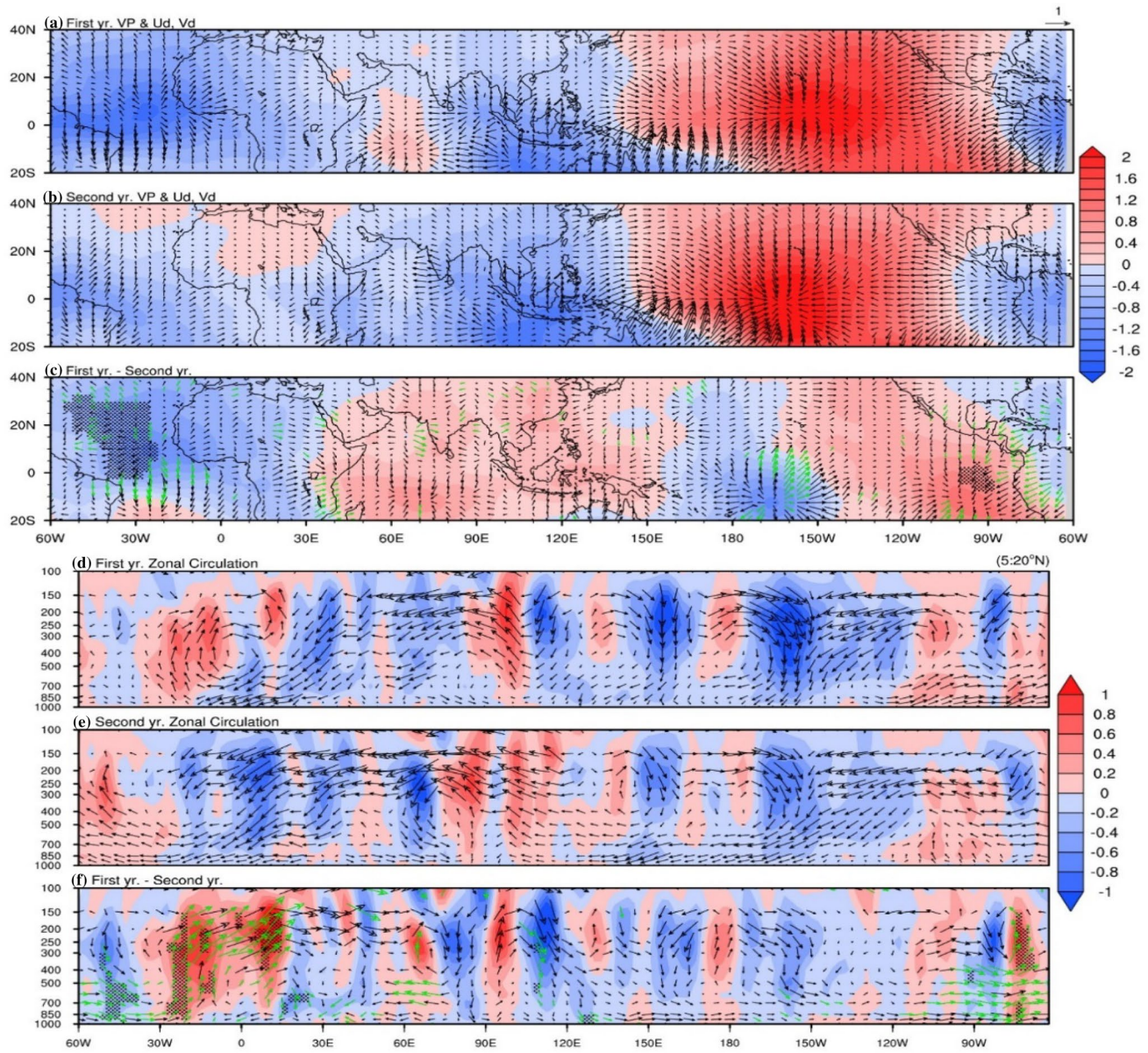

Fig. 5 **a** and **b** Composite of JJA 200 hPa velocity potential anomalies (shaded; $\times 10^6$ m^2/s) overlaid with divergent components of wind anomalies (vectors; m/s). **d** and **e** Composite of JJA zonal circulation over the northern hemispheric tropical region (5°N–20°N) with speed in the vertical direction (shaded; *0.05 m/s) and zonal vertical velocity (vector; m/s), with common scaling as mentioned. **a** and **d** For the 1st year, **b** and **e** for the 2nd year. **c** Differences in 1st year and 2nd year for velocity potential (shaded) at 85% confidence level (black dots), divergent components (black vectors) at 85% confidence level (green vectors). **f** Differences in 1st year and 2nd year for vertical speed (shaded) at 85% confidence level (black dots), zonal vertical velocity (black vectors) at 85% confidence level (green vectors)

only during the first winter but also in the second, during multi-year La Niña cases.

As mentioned earlier, the presence of warm SST anomalies corresponds to the Atlantic Niño in the first year (Fig. 2) intensifies the Inter Tropical Convergence Zone (ITCZ) and enhances the upper-tropospheric divergence over the equatorial east Atlantic and West Africa (Fig. 4). This shoves the upper tropospheric GPH poleward over North Africa with successive meridional negative, positive and negative GPH anomalies from the tropics to extra-tropics (Fig. 6a). These results are consistent with Yadav (2017) and Yadav et al. (2018). They found that the negative GPH anomaly formed over north-west Europe due to Atlantic Niño warming could impose positive GPH anomaly in central Asia by the Eurasian Rossby wave-train dispersion. Figure 6 also shows the Rossby wave activity flux (WAF) (yellow arrows) which is the preferred region for the propagation of a strong Rossby wave train. It is zonally oriented from North

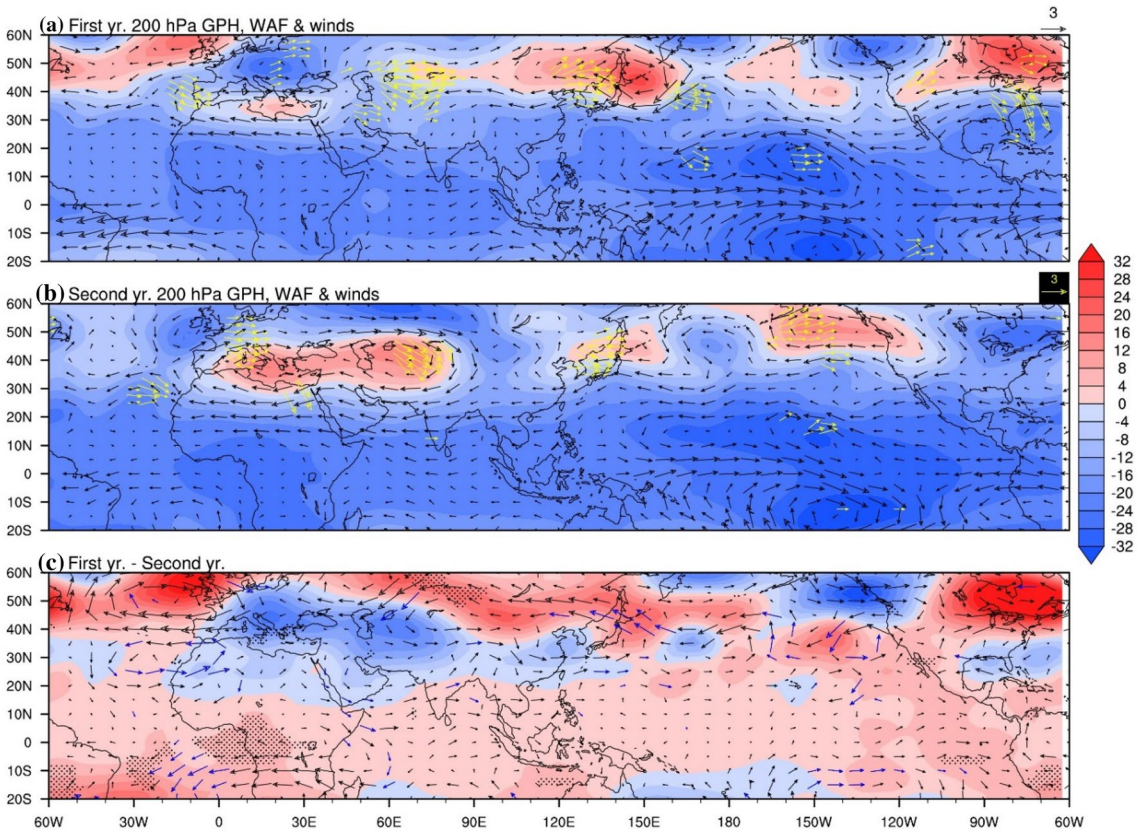

Fig. 6 **a** and **b** Composite of JJA 200 hPa geopotential height anomalies (shaded; m) overlaid with 200 hPa wind anomalies (black vectors; m/s) and Rossby WAF (yellow vectors; m^2/s^2) depicting the preferred path for the wave train, with scaling as mentioned. **a** For the 1st year, **b** same as in **a**, but for the 2nd year. **c** Differences in 1st year and 2nd year for geopotential height (shaded) at 85% confidence level (black dots) and 200 hPa wind anomalies (black vectors) at 85% confidence level (blue vectors)

America towards central Asia via north Atlantic and northwest Europe. As a result, anomalous positive GPH values are noted over the central Asian region. Positive GPH anomalies are associated with anomalous anticyclonic circulation and anomalous easterlies to the south of its center. These strong easterly winds in the sub-tropical westerly jet's core-zone indicates weakening of the Asian Jet (Yadav et al. 2018) as illustrated in Fig. 7a. They suggested that the weak Asian subtropical westerly jet east of the Caspian Sea, reduces the upper-tropospheric divergence towards the Indian subcontinent and is the cause for below normal Indian summer monsoon. In response to the Atlantic Niño, a weak westerly Asian Jet around 45°N is evident in Fig. 7c. Difference in 200 hPa winds between the first and the second year shows an anomalous cyclonic circulation pattern over the Caspian Sea region. This supports the reduced upper-tropospheric divergence over the Indian subcontinent and contributes for reduced rainfall over the north-western parts of India. This allows the penetration of westerly troughs into the eastern and central Himalayan regions. As it interacts with the lower-level monsoon flow, the monsoon trough shifts northwards towards the Himalayas, as observed in the Fig. 3a, d.

Strong positive GPH anomalies corroborated by anticyclonic circulation is seen north of Meiyu-Baiyu rain band, as part of Rossby wave guide (known as westerly wave) during the first year. Anomalous easterly winds to the south of this positive GPH suggests the weakening of subtropical westerly jet. Further, these GPH anomalies reduce the climatological background pressure gradient between tropics and midlatitude, which is responsible for the weakening of westerly jet (e.g., Yadav et al. 2018). In general, the intensified westerly jet in the upper troposphere (500–200 hPa) could enhance the atmospheric convection over the Meiyu/Baiyu rain band by advecting warm temperatures from the Tibetan plateau region (e.g., Sampe and Xie 2010). However, weakening of subtropical westerly jet in the first year is partly responsible for the reduced rainfall over the Meiyu-Baiyu rain band region, which includes north-east China, Korea and Japan (Fig. 3). This suggests the impact of La Niña and Atlantic Niño in inducing atmospheric anomalies over both the south and East Asia regions. Further, the Rossby wave activity flux embedded within the PNA pattern also seems to contribute to the strengthening of negative GPH anomaly formed over north-west Europe, apart from the Atlantic Niño's

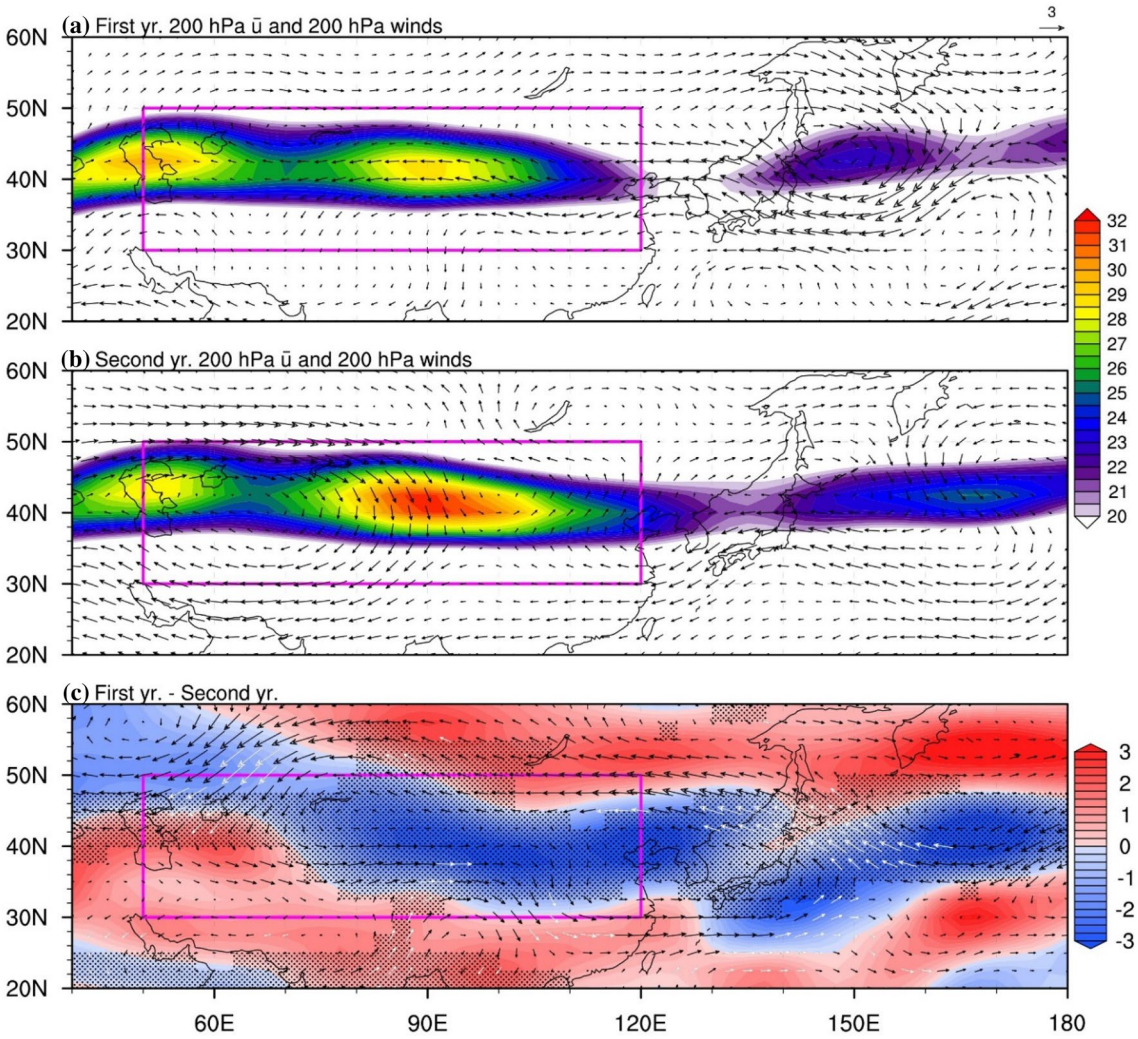

Fig. 7 **a** and **b** Composite of JJA 200 hPa zonal westerly winds (shaded; > 20 m/s), with scaling as mentioned. The box depicts the location of the Asian subtropical westerly jet. **a** For the 1st year, **b** same as in **a**, but for the 2nd year. **c** Differences in 1st year and 2nd year for zonal westerly winds (shaded) at 99.99% confidence level (black dots) and 200 hPa wind anomalies (black vectors) at 85% confidence level (white vectors)

impact. This suggests possible influence of the PNA pattern on the south and East Asian summer monsoons along with the Atlantic Niño. Difference between the first and second years further supports the presence of a wave pattern along the subtropical westerly jet and adjustments in the circulation patterns. This clearly supports the first year's rainfall over northern parts of India and the Meiyu/Baiyu rain band regions (Figs. 3c, 6c).

In the second year, the wave train stretches poleward over the north-east Pacific and North American regions as illustrated in the GPH anomalies (Fig. 6b, c) and these anomalies are weak over the north Atlantic region. At the same time, anomalous upper level anticyclonic circulation with positive GPH anomalies extending from central Asia to Mediterranean Sea region centered around 40°N is apparent in the second year, which depicts a stronger south Asian monsoon. The GPH anomalies over the Meiyu/Baiyu rain band region is weaker in the second year compared to the first year. Further, the anomalous northern hemispheric upper level cyclonic circulation, in response to the equatorial Pacific cooling, extends far west up to 130°E. The resultant shift in convective bands towards the Indian Ocean supports enhanced rainfall over most of the parts of South Asia. This westward extension of upper level cyclonic circulation is much less in first year as compared to second year. This analysis suggests that the representation of both the Atlantic Niño and La Niña related SST anomalies in coupled models are important in order to obtain better teleconnections to the south Asian and East Asian summer rainfalls.

5 Assessment of CMIP5 models

It is found from the observations, that the Indian summer monsoon (ISM) rainfall is low (high) during the first (second) year of multiyear La Niña events. The East Asian rainfall pattern also displayed large differences between the first and second years. In order to improve the representation of the summer rainfall over south and east Asia, it is essential to capture the ENSO-monsoon rainfall teleconnections correctly in coupled models (e.g., Ramu et al. 2016; Chowdary et al. 2017). Apart from ENSO, Atlantic Niño can also influence the summer monsoon rainfall over south Asia (e.g., Yadav 2017). Analysis of observations suggested that, the Atlantic Niño has co-occurred with La Niña in the first year and is absent in the second year. Thus, it is interesting and important to know the credibility of the current coupled models in capturing both Atlantic Niño as well as multiyear La Niña events and their teleconnections to the south and east Asian summer monsoons. It is noted that only 9 out of 38 models are able to simulate the oceanic conditions during multiyear La Niña events for the period of 1901–2005. Models which represent 4 or more events are considered for the analysis. The selected models are highlighted in Table 1.

Figure 8 shows the composite of SST, SLP and 850 hPa wind anomalies over the tropical region during the first years for selected individual models. It is seen that in the first year, La Niña conditions are simulated well in all the models, though models such as CCSM4, GFDL-ESM2M, MIROC5 and MPI-ESM-P overestimate the cold anomalies. The anomalous warming in the east equatorial Atlantic Ocean is simulated in three models. Only MIROC5 (Fig. 8f) has simulated the basin-wide significant cooling of the Indian Ocean. At the same time, warm anomalies have also been depicted in the eastern Indian Ocean. This may be due to the overestimation in the expanse of La Niña in the Pacific Ocean. Except models like CCSM4, CMCC-CM, all other models display westward extension of La Niña related cold anomalies over the equatorial Pacific unlike in the observations (Fig. 2). This unrealistic westward extension of equatorial Pacific SST anomalies could modulate teleconnections to the south and East Asian region (e.g., Song et al. 2014; Li and Xie 2014; Ramu et al. 2018). Many climate models simulate an excessive cold tongue in the mean state, that extends too far westward in the equatorial Pacific (e.g., Yu and Mechoso 1999; Li and Xie 2012). This excessive westward cold tongue, in general, modulates the convection over the western Pacific warm pool in the models (e.g., Li et al. 2015). As a result, the SST-convective feedback becomes

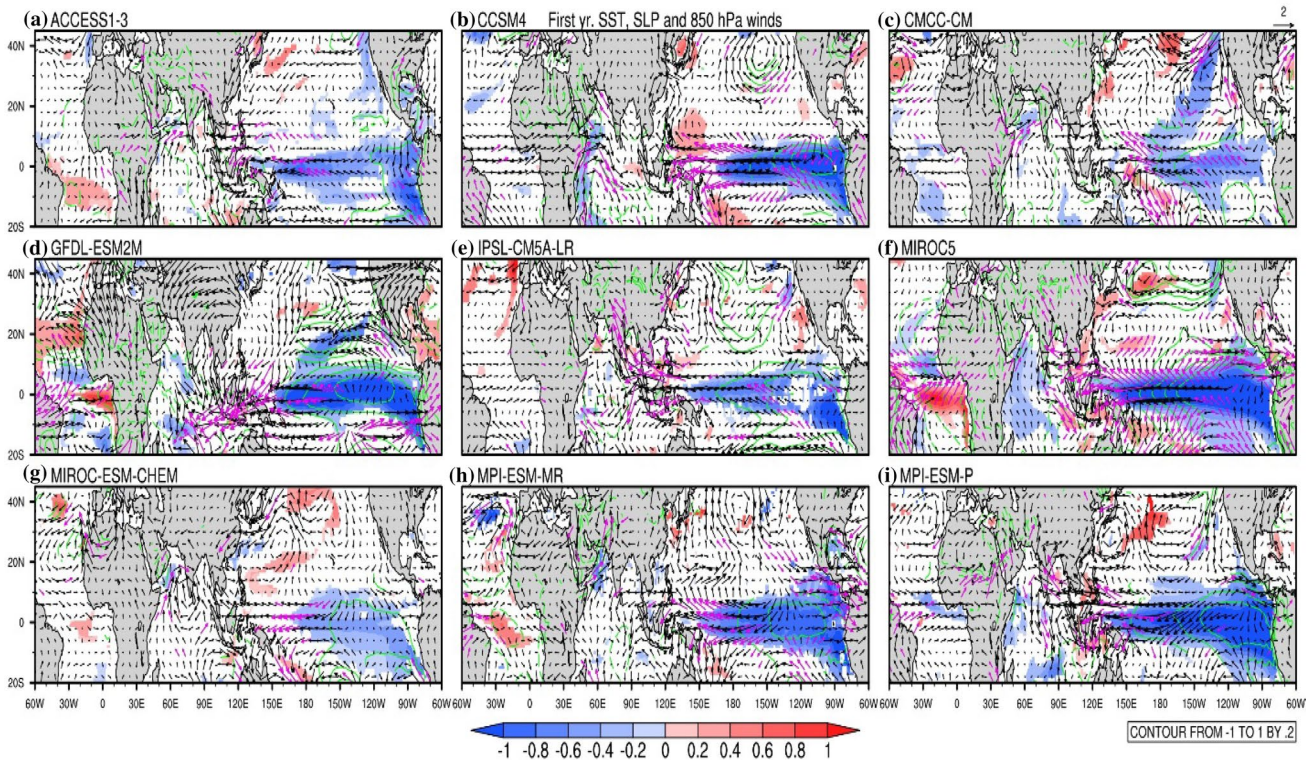

Fig. 8 Composite of JJA SST anomalies (shaded; °C) overlaid with seasonal SLP anomalies (green line contours; hPa) at 85% confidence level and 850 hPa wind anomalies (black vectors; m/s) at 85% confidence level (magenta vectors; m/s) for the 1st year

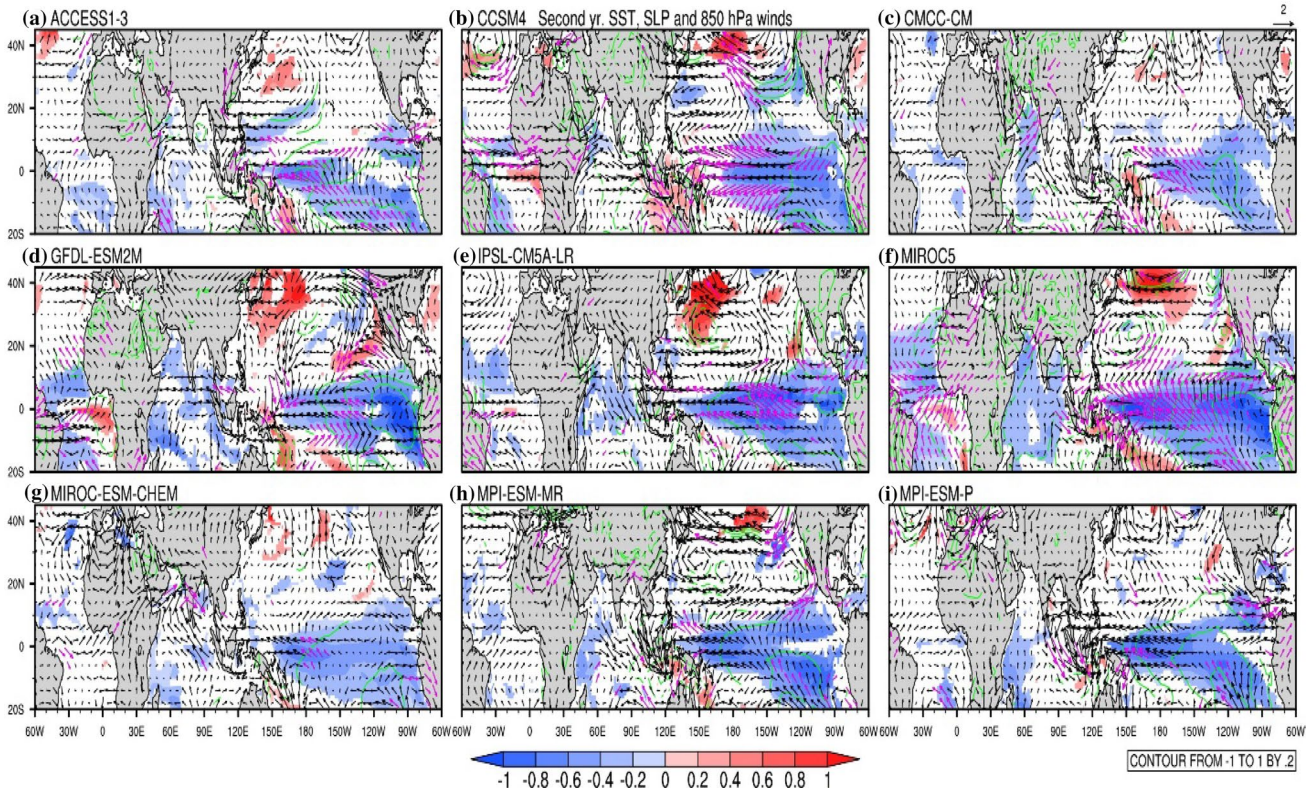

Fig. 9 Similar to Fig. 8, but for the 2nd year

weak and facilitates the SST warming in the equatorial western Pacific causing for the development of La Niña-like Pattern (Li et al. 2016). These western Pacific SST anomalies in those models can affect the Asian summer monsoon rainfall via a Gill-type Rossby wave response (Li et al. 2017). In the second year, there is a reduction in the simulated intensities of La Niña related SST anomaly magnitudes (Figs. 2, 9). This is true for all the models except MIROC-ESM-CHEM (Figs. 8g, 9g), where intensified La Niña is seen in the second year. The weak positive anomalies in the second year over equatorial Atlantic Ocean is simulated by IPSL-CM5A-LR, MIROC5, GFDL-ESM2M, CCSM4, which is not seen in the observations. The cooling over the Indian Ocean is depicted by three models such as GFDL-ESM2M, IPSL-CM5A-LR and MIROC5, in varying proportions. Similar to the first year, many models display westward extension of the equatorial Pacific cold SST anomalies in the second year as well. This unrealistic pattern in SST anomalies might influence monsoon rainfall in the models.

All the models (except MIROC-ESM-CHEM—Fig. 8g) shows basin wide reduced SLP anomalies over the Indian Ocean in the first year unlike in the observations. This low SLP is accompanied by convergence of low-level winds over most of the Indian Ocean and ISM regions, which is in fact much weaker in the observations. This low level convergence supports strong rainfall anomalies in models over the ISM region during the first year (Fig. 10). Further, many models show eastward extension of negative SLP anomalies toward the northwest Pacific, which is absent in the observations. This unrealistic SLP patterns corroborated by SST anomalies distribution over the Indo-Pacific region are mainly responsible for the misplacement of low level circulation anomalies. This in-turn would trigger the rainfall patterns in the monsoon region. For example, a weak anticyclone over the northwest Pacific and cyclonic circulation south of Japan are evident in the observations (Fig. 4). This is important for maintaining the tri-pole pattern in the East Asian monsoon rainfall region (Fig. 3). However, some models completely missed both the anticyclonic as well as cyclonic circulations over northwest Pacific and the associated rainfall patterns (Figs. 8, 10). Anticyclonic circulation over the northwest Pacific is seen in models like ACCESS1-3 and MPI-ESM-P but far too extended to the west or north. Only four models ACCESS1-3, GFDL-ESM-2M, MIROC5, MPI-ESM-MR are able to depict the reduced SLP anomalies associated with the Atlantic Niño. However, the impact of Atlantic Niño on south and East Asian monsoon is not well established in the models. This will be discussed in latter stage of this study. The large scale circulations such as

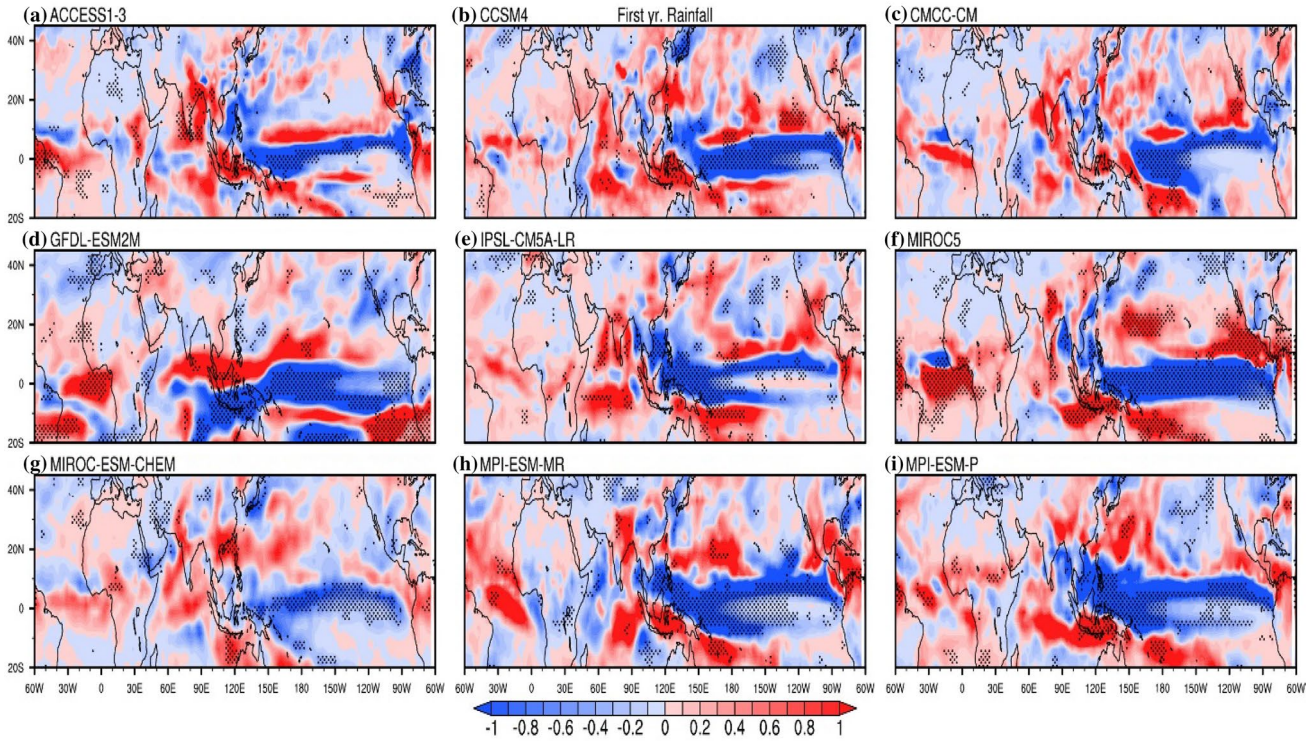

Fig. 10 Composite of JJA normalized rainfall anomalies (shaded) overlaid with rainfall anomalies at 85% confidence levels (dots) for the 1st year

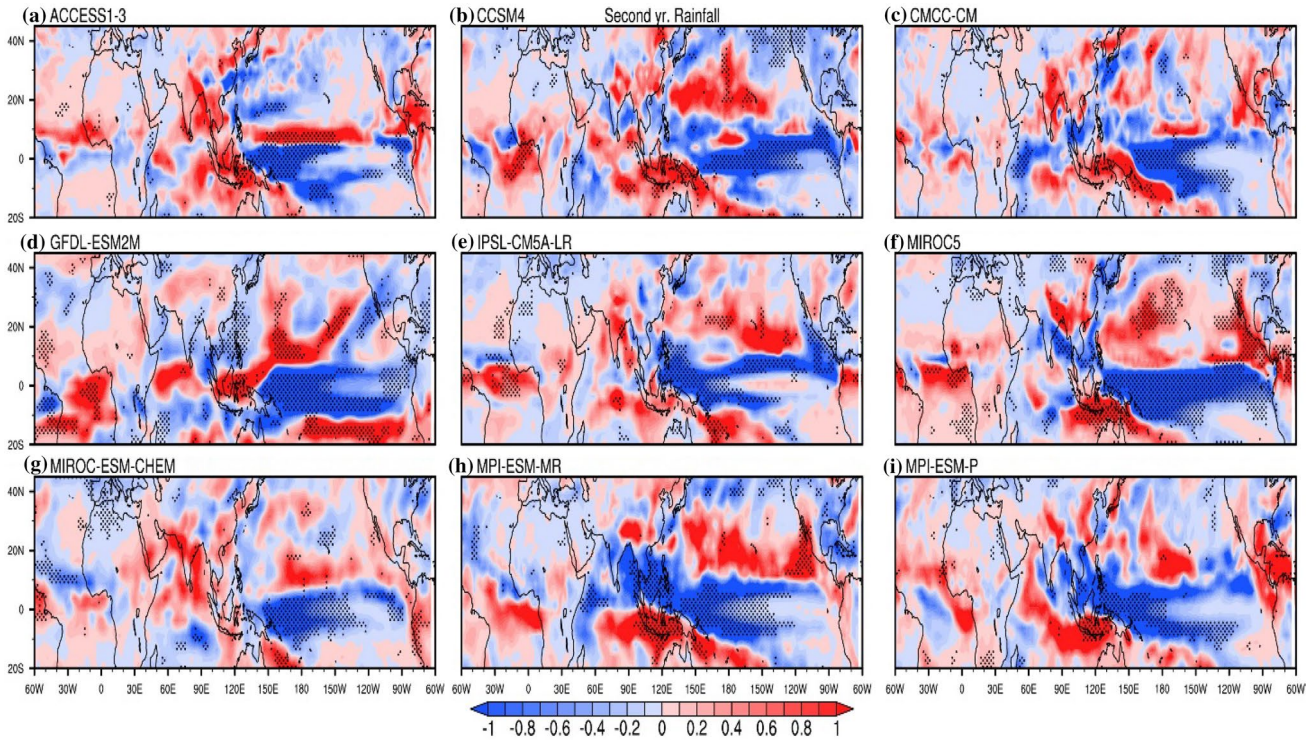

Fig. 11 Similar to Fig. 10, but for the 2nd year

200 hPa divergent wind and velocity potential associated with the La Niña events, monsoons and Atlantic Niño are examined.

It is noted that nearly half of the models (ACCESS, CMCC-CM, IPSL-CM5A-LR, MIROC-ESM-CHEM) are able to simulate the positive rainfall anomalies over India in the second year (Fig. 11). Among these models only ACCESS1-3 displayed the tri-pole pattern rainfall anomalies over the East Asian region as in the observations. Similar to the first year, negative SLP anomalies are strong over the TIO and south Asian region except in models such as GFDL-ESM2M, MIROC-ESM-CHEM (Fig. 9). Weak cyclonic circulation over the Bay of Bengal and adjacent Indian land mass is seen some models. Low SLP over south Asian region due to La Niña and associated local cyclonic circulation have caused for the excess rainfall over India and these circulations features are well captured in some models (ACCESS1-3, CMCC-CM, IPSL-CM5A-LR and MIROC-ESM-CHEM). Misrepresentation of East Asian rainfall in all other models is due to the extension of low SLP from Indian Ocean to the northwest Pacific. Positive SLP anomalies over the equatorial Pacific extended to the west in most of the models, which is mainly associated with the extension of negative SST anomalies related to the second year La Niña event. Overall, the first year rainfall patterns in south and East Asia are not well represented in most of the models. Whereas, in the second year, the monsoon rainfall over India is well depicted in many models but East Asian monsoon rainfall patterns are represented only by one model (MPI-ESM-P). This difference in teleconnection in the first and second years are mainly due to the misrepresentation of SST anomalies in the tropics and the associated modulation in the circulation patterns unlike in the observations.

In the first year, strong upper level convergence over the central Pacific Ocean corresponding to La Niña is seen in observations and few models (Fig. 12). This convergence is shifted westward in many models. On the other hand, upper level convergence and negative velocity potential are seen in the south equatorial Indian Ocean and equatorial Atlantic regions, respectively in the observation (Fig. 5). A weak divergence is also evident over the monsoon region. It is important to note that none of these models are able to represent the maximum divergence zones correctly. This indicates that the misrepresentation of large-scale circulation in the first year also contributed to unorganized rainfall patterns over the south and east Asia region. In the second year, four models (ACCESS1-3, CMCC-CM, IPSL-CM5A-LR and MIROC-ESM-CHEM) represented the upper level

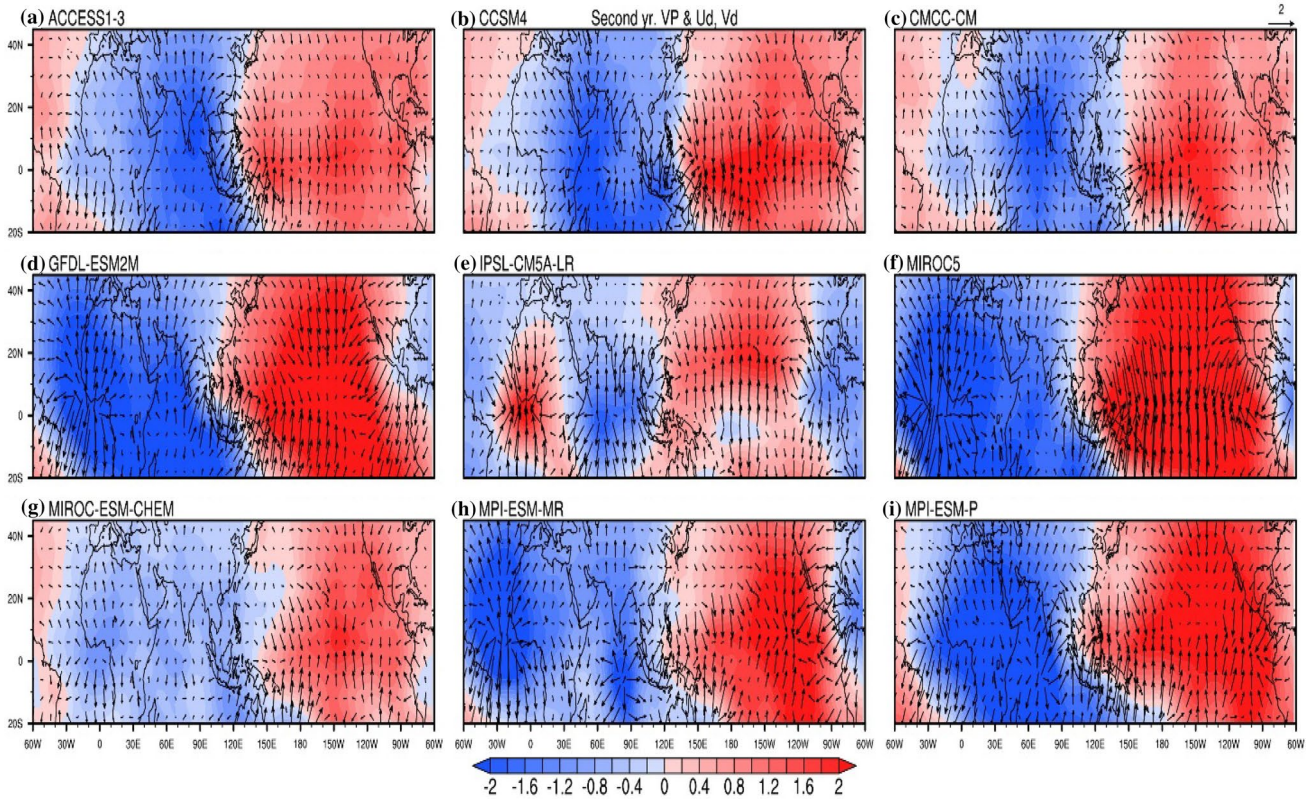

Fig. 12 Composite of JJA 200 hPa velocity potential anomalies (shaded; $\times 10^{-6}$ m^2/s) overlaid with anomalous divergent component of winds (vectors; s^{-1}), with scaling as mentioned for the 1st year

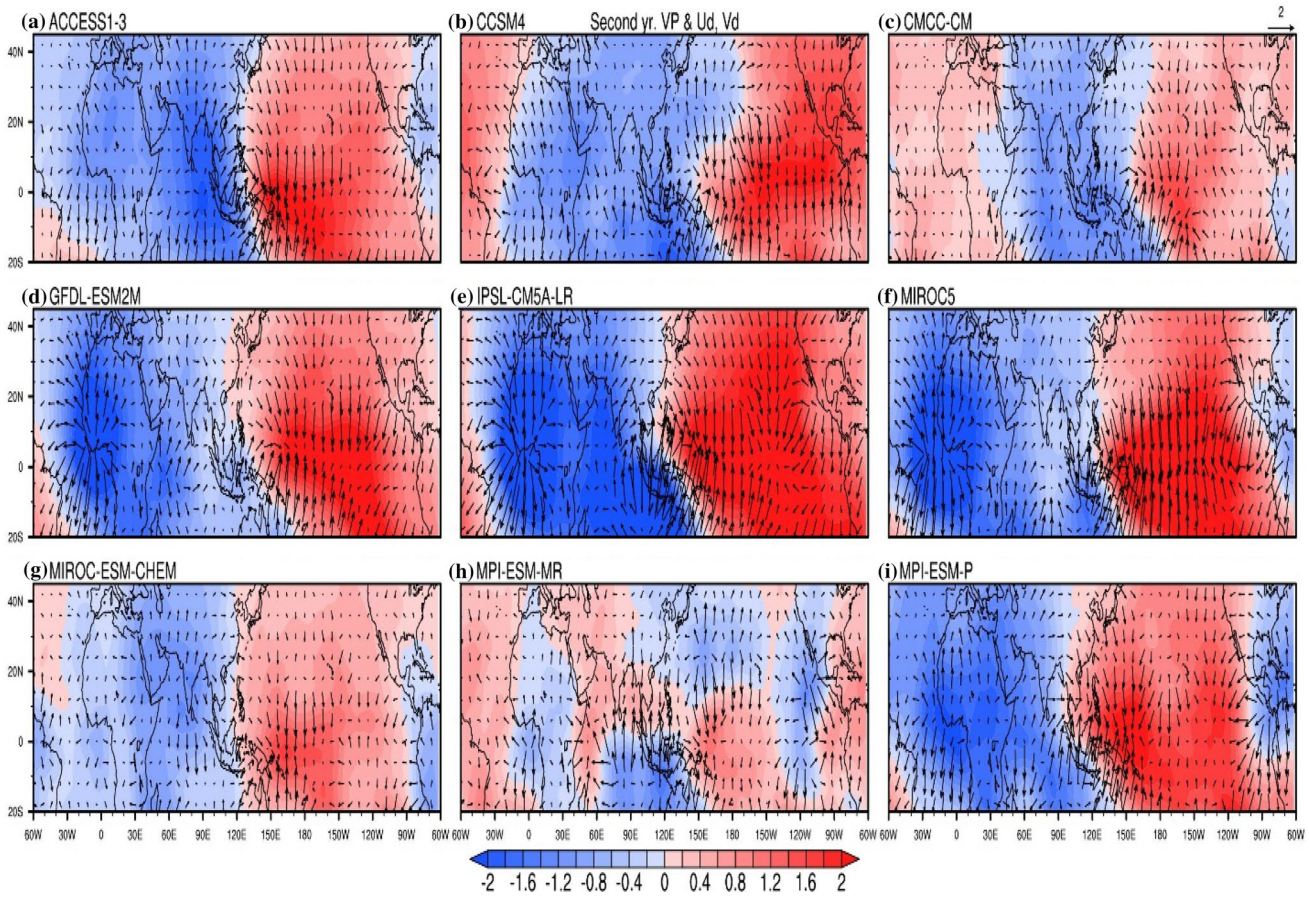

Fig. 13 Similar to Fig. 12, but for the 2nd year

divergence well over the Indian Ocean and monsoon region when compared to the observations (Fig. 13). In rest of the models, the upper-level convergence or divergence centers are misrepresented and thus the rainfall patterns are slightly misplaced.

In all the models during the first year (Fig. 14), weak PNA pattern arising from the central Pacific cooling is apparent. Very weak pair of equatorial upper level cyclonic circulations, which triggers the poleward alternating negative-positive-negative GPH anomalies supports this. The northward meridional wave over the African longitudes associated with Atlantic Niño is weak/not seen in models. Since the meridional wave train is missing, the weakening of the Asian jet is not captured in models (Fig. 16). This is also apparent in the wave activity flux in the models (Fig. 14) compared to the observations. A strong upper level anticyclonic circulation oriented to the east of the Caspian Sea adds to the zonal flow of the westerlies in the models unlike in the observations. In the second year, the GPH anomalies are negative throughout tropics in both observations and model (Figs. 6, 15, 16). In the subtropics, the negative and positive GPH anomalies are not represented systematically in the models and as a result, the predominant westerly flow is seen (Fig. 17). The preferred path for the wave is seen all along the subtropical belt, compared to only a few pockets in the observations. The models are unable to simulate the single elongated anticyclonic circulation over the Mediterranean Sea—west Asian region. Overall, the skill of coupled models in capturing Atlantic Niño teleconnections to south Asian region is poor (e.g., Kucharski and Joshi 2017; Yadav et al. 2018).

6 Summary and conclusions

Impact of multi-year La Niña events on South and East Asian summer monsoon rainfall are examined in observations and CMIP5 models. We have identified four 2-year/multiyear La Niña events during the period of 1948–2016. Composite analysis of SST anomalies suggests that, the La Niña related cooling is slightly shifted towards the south and south-central Pacific Ocean region in the second year. An Atlantic Niño like pattern is evident in the first year summer, but not in the second year summer. Note that the presence of Atlantic Niño in the first year (JJA) can contribute

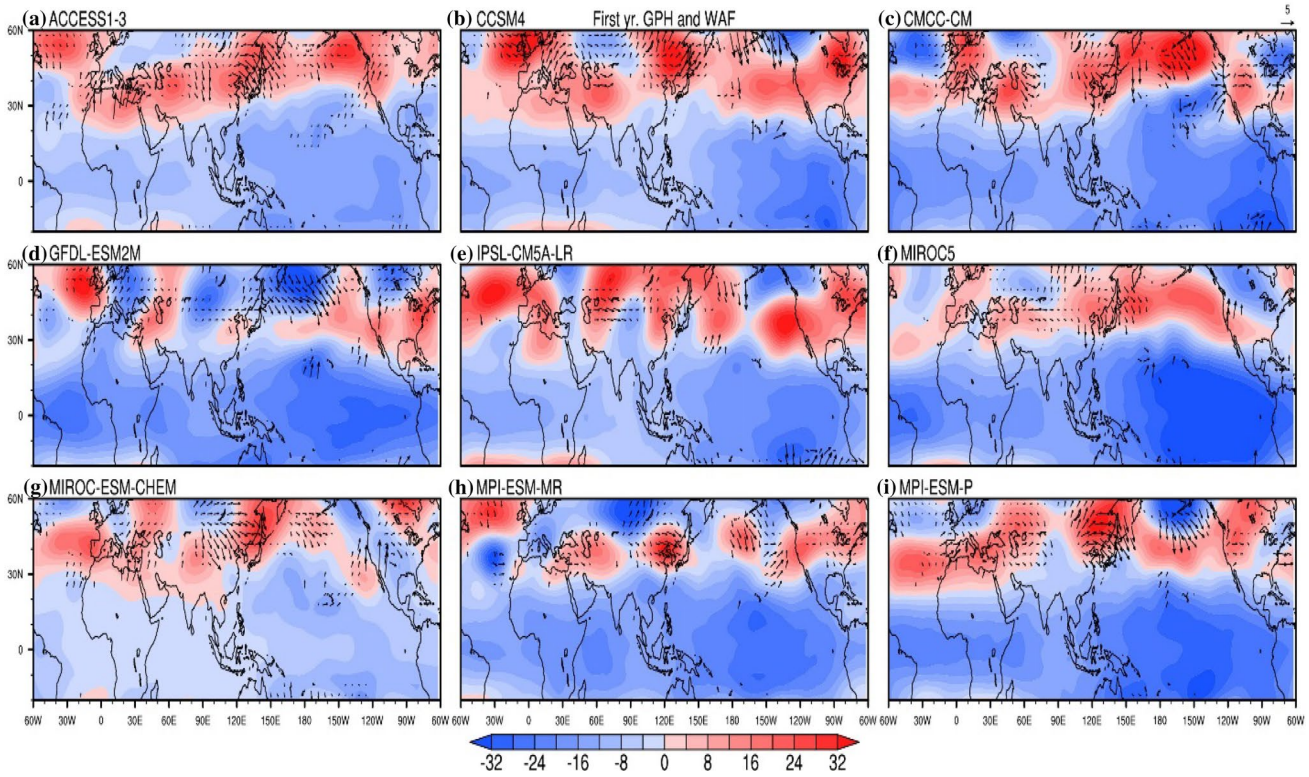

Fig. 14 Composite of JJA 200 hPa geopotential height anomalies (shaded; m) overlaid with WAF anomalies (vectors; m^2/s^2), with scaling as mentioned, for the 1st year

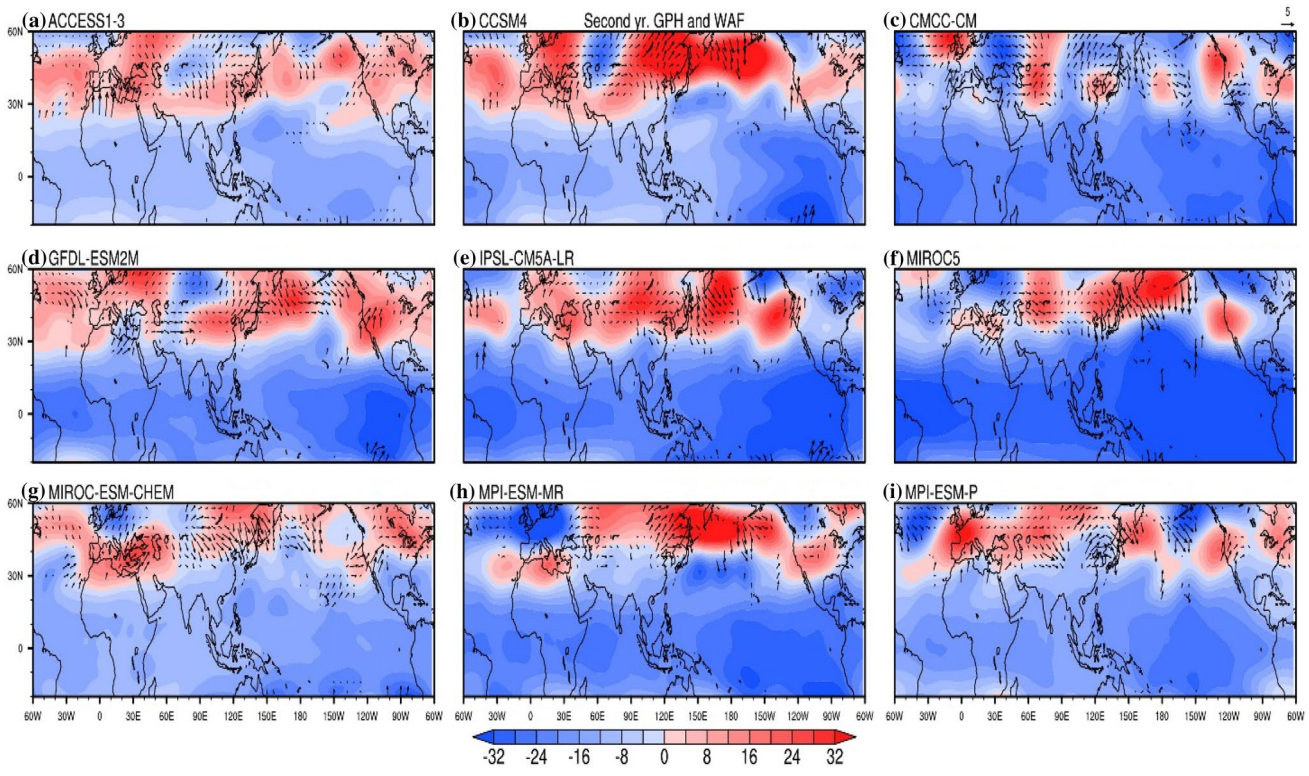

Fig. 15 Similar to Fig. 14, but for the 2nd year

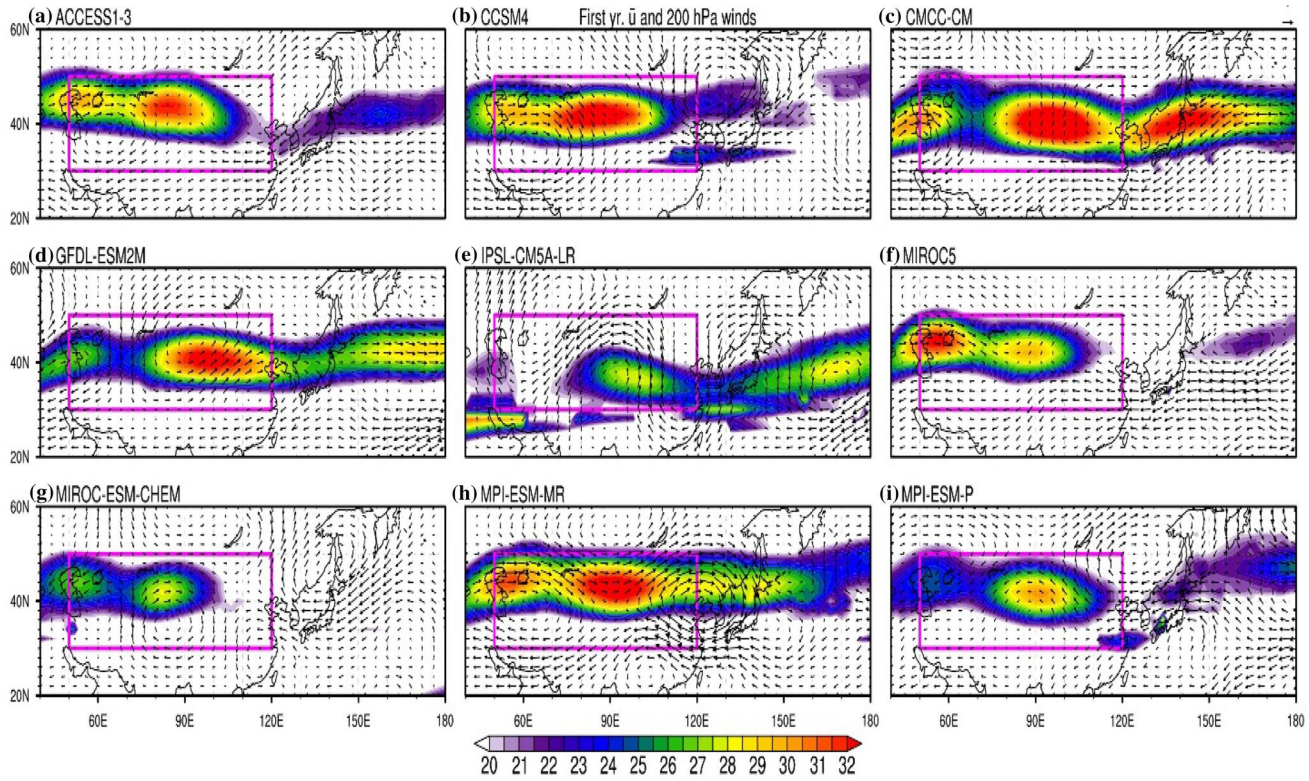

Fig. 16 Composite of JJA 200 hPa mean zonal winds (shaded; m/s) overlaid with seasonal wind anomalies (vectors; m/s), with scaling as mentioned, for the 1st year. The box denotes the mean location of the location of the Asian subtropical westerly jet

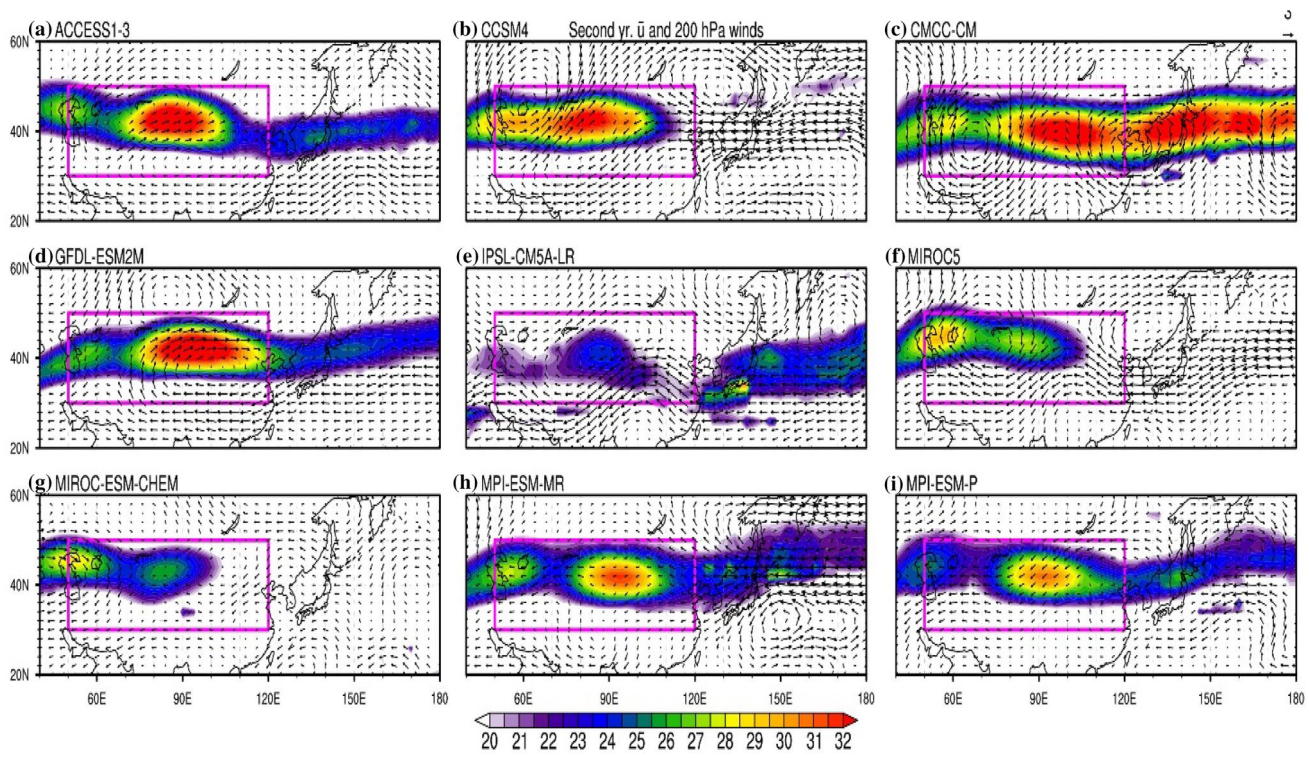

Fig. 17 Similar to Fig. 16, but for the 2nd year

to the persistent of a strong La Niña in the Pacific, by the subsequent boreal winter. Few studies have identified that the Atlantic Niño attains its peak phase, when the Pacific La Niña is in its developing phase (e.g., Haarsma and Hazeleger 2007; Wang 2002). In response to the Atlantic Niño, using partially-coupled model experiments and observations, Rodriguez-Fonseca et al. (2009) reported the manifestation of an anomalous Walker circulation with the ascending branch over the Atlantic and the descending branch over the central Pacific. They suggested that the subsidence, enhances the surface divergence in the equatorial Pacific shallows the equatorial thermocline. The Bjerknes feedback helps in the persistent of full La Niña conditions by boreal winter. Central TIO is cooler during the first year whereas the northern Indian Ocean is cooler in the second year. In the first (second) year, negative (positive) rainfall anomalies are apparent over most of the South Asian countries except Bangladesh and Sundarbans. In addition, a tri-pole like structure in rainfall anomalies is reported in the East Asian Monsoon region with positive anomalies over southern and central China and negative over parts of Myanmar, Thailand and Cambodia regions and north-east China—North Korea in the first year and vice-versa in the second year.

Analysis reveals distinct evolution of atmospheric teleconnections to the south and East Asian precipitation anomalies during multiyear La Niña events. In the first year, moisture convergence corroborated by low-level circulation to the north of Bangladesh and central India supports the positive rainfall anomalies. The negative VIM anomalies in the rest of the subcontinent are in line with the negative rainfall anomalies. In case of the second year, anomalous low-level cyclonic circulation over central Bay of Bengal enhanced the moisture transport into the Indian subcontinent and hence results in positive rainfall anomalies. This is also seen in the positive VIM anomalies over the subcontinent. A tri-pole structure in the VIM anomalies is seen in the East Asian monsoon region. This tri-pole like structure supports the similar rainfall anomalies during the second year. The reversed tri-pole structure in rainfall anomalies is not reflected in the VIM anomalies during the first year, although, anomalous negative VIM over Cambodia and Thailand are consistent with the negative rainfall anomalies during the same time. Weak positive VIM and southeasterlies associated with the northwest Pacific anticyclone in central-eastern China and South Korean region support positive rainfall anomalies. Likewise, the changes in moisture transport and low-level circulation explained the rainfall patterns in the second year over East Asian region. Moreover, an anomalous upper level divergence extends from southeast Indian Ocean to the Indian subcontinent as a response to La Niña in the second year. This response is found to be weak in the first year. This clearly suggests that enhanced rainfall over the South Asian region is influenced remotely by La Niña in addition to local circulation changes during both the years.

In addition to these changes, the Atlantic Niño has also been found to be remotely influencing the South Asian rainfall during the first year. The SST warming associated with Atlantic Niño intensifies the ITCZ, and enhances the upper-tropospheric divergence over equatorial east Atlantic and West Africa. This shoves the upper tropospheric GPH poleward over North Africa with successive meridional negative, positive and negative GPH anomalies from the tropics to extra-tropics. This triggers positive GPH anomaly accompanied by anticyclonic circulation in central Asia due to the dispersion of the Eurasian Rossby wave-train. This is also supported by Rossby wave activity flux. Anomalous easterlies to the south of its center weaken the sub-tropical westerly jet, which in turn reduces the upper-tropospheric divergence towards the Indian subcontinent. It also contributes for the below (above) normal rainfall over Indo-Pakistan (south-east Tibetan Plateau) region.

We have further examined the ability of CMIP5 models in representing multiyear La Niña teleconnections to the south and East Asian summer monsoons. Only 9 out of 38 models are able to represent multiyear La Niña events. Most of these models have simulated westward extended intense cold SST anomalies over the equatorial Pacific, which were not present in the observations for both the years. Some models are able to reproduce the south Asian rainfall and circulation anomalies well in the second year, but, failed to do so in the first year. Almost all the models depict strong convergence and negative SLP anomalies over the ISM region and Indian Ocean during the first year, which is not seen in the observations. However, few models completely missed the circulation features over the northwest Pacific during both the years. These circulations are important in maintaining the tri-pole structure in rainfall of East Asia. The impact of Atlantic Niño on the Asian rainfall is not well established in these models. None of the models are able to represent the maximum upper-level divergence zones correctly during the first year. The convergence zone over the western Indian Ocean is also missed in models. During the second year, few of the models are able to represent the upper level divergence over south Asia and this supports positive rainfall over this region. However, unrealistic Atlantic Niño like SST anomalies are seen in some models during second year. Overall, CMIP5 models showed limited skill in representing multiyear La Niña events including second year summer SST cooling in the equatorial Pacific and associated teleconnections.

Acknowledgements We wish to acknowledge the support of ESSO-IITM, MoES. We thank the anonymous reviewers for their comments/

suggestions which have helped us to improve the manuscript. Inputs and help from Dr. Aditi Deshpande, Savitribai Phule Pune University are also acknowledged. NCL has been used for preparing the manuscript figures.

References

Alexander MA, Bladé I, Newman M, Lanzante JR, Lau NC, Scott JD et al (2002) The atmospheric bridge: the influence of ENSO teleconnections on air–sea interaction over the global oceans. J Clim 15(16):2205–2231. https://doi.org/10.1175/1520-0442(2002)015%3C2205:TABTIO%3E2.0.CO;2

Andrews ED, Antweiler RC, Neiman PJ, Ralph FM (2004) Influence of ENSO on flood frequency along the California coast. J Clim 17(2):337–348. https://doi.org/10.1175/1520-0442(2004)017%3C0337:IOEOFF%3E2.0.CO;2

Angell JK (1981) Comparison of variations in atmospheric quantities with sea surface temperature variations in the equatorial eastern Pacific. Mon Weather Rev 109(2):230–243. https://doi.org/10.1175/1520-0493(1981)109%3C0230:COVIAQ%3E2.0.CO;2

Baohua R, Ronghui H (1999) Interannual variability of the convective activities associated with the East Asian summer monsoon obtained from TBB variability. Adv Atmos Sci 16(1):77–90. https://doi.org/10.1007/s00376-999-0005-4

Barlow M, Cullen H, Lyon B (2002) Drought in central and southwest Asia: La Niña, the warm pool, and Indian Ocean precipitation. J Clim 15(7):697–700. https://doi.org/10.1175/1520-0442(2002)015%3C0697:DICASA%3E2.0.CO;2

Bhalme HN, Mooley DA, Jadhav SK (1983) Fluctuations in the drought/flood area over India and relationships with the southern oscillation. Mon Weather Rev 111(1):86–94. https://doi.org/10.1175/1520-0493(1983)111%3C0086:FITDAO%3E2.0.CO;2

Boening C, Willis JK, Landerer FW, Nerem RS, Fasullo J (2012) The 2011 La Niña: so strong, the oceans fell. Geophys Res Lett. https://doi.org/10.1029/2012GL053055

Chen M, Li T, Shen X, Wu B (2016) Relative roles of dynamic and thermodynamic processes in causing evolution asymmetry between El Niño and La Niña. J Clim 29(6):2201–2220. https://doi.org/10.1175/JCLI-D-15-0547.1

Choi K-Y, Vecchi GA, Wittenberg AT (2013) ENSO transition, duration, and amplitude asymmetries: role of the nonlinear wind stress coupling in a conceptual model. J Clim 26(23):9462–9476. https://doi.org/10.1175/JCLI-D-13-00045.1

Chowdary JS, Harsha HS, Gnanaseelan C, Srinivas G, Parekh A, Pillai P, Naidu CV (2017) Indian summer monsoon rainfall variability in response to differences in the decay phase of El Niño. Clim Dyn 48(7–8):2707–2727. https://doi.org/10.1007/s00382-016-3233-1

Deppenmeier AL, Haarsma RJ, Hazeleger W (2016) The Bjerknes feedback in the tropical Atlantic in CMIP5 models. Clim Dyn 47(7–8):2691–2707. https://doi.org/10.1007/s00382-016-2992-z

DiNezio PN, Deser C (2014) Nonlinear controls on the persistence of La Niña. J Clim 27(19):7335–7355. https://doi.org/10.1175/JCLI-D-14-00033.1

DiNezio PN, Deser C, Karspeck A, Yeager S, Okumura Y, Danabasoglu G, Rosenbloom N, Caron J, Meehl GA (2017a) A 2 year forecast for a 60–80% chance of La Niña in 2017–2018. Geophys Res Lett 44(22):11624–11635. https://doi.org/10.1002/2017GL074904

DiNezio PN, Deser C, Okumura Y, Karspeck A (2017b) Predictability of 2-year La Niña events in a coupled general circulation model. Clim Dyn 49(11–12):4237–4261. https://doi.org/10.1007/s00382-017-3575-3

Feng L, Zhang R-H, Wang Z, Chen X (2015) Processes leading to second-year cooling of the 2010–12 La Niña event, diagnosed using GODAS. Adv Atmos Sci 32(3):424–438. https://doi.org/10.1007/s00376-014-4012-8

Frauen C, Dommenget D (2010) El Niño and La Niña amplitude asymmetry caused by atmospheric feedbacks. Geophys Res Lett. https://doi.org/10.1029/2010GL044444

Gill AE (1980) Some simple solutions for heat-induced tropical circulation. Q J R Meteorol Soc 106(449):447–462. https://doi.org/10.1002/qj.49710644905

Gill AE, Rasmusson EM (1983) The 1982–1983 climate anomaly in the equatorial Pacific. Nature 306(5940):229–234. https://doi.org/10.1038/306229a0

Godfred-Spenning CR, Reason JC (2002) Interannual variability of lower-tropospheric moisture transport during the Australian monsoon. Int J Climatol 22(5):509–532. https://doi.org/10.1002/joc.710

Gordon AL, Fine RA (1996) Pathways of water between the Pacific and Indian Oceans in the Indonesian seas. Nature 379(6561):146–149. https://doi.org/10.1038/379146a0

Haarsma RJ, Hazeleger W (2007) Extratropical atmospheric response to equatorial Atlantic cold tongue anomalies. J Clim 20(10):2076–2091. https://doi.org/10.1175/JCLI4130.1

Harris I, Jones PD, Osborn TJ, Lister DH (2014) Updated high-resolution grids of monthly climatic observations—the CRU TS3.10 dataset. Int J Climatol 34(3):623–642. https://doi.org/10.1002/joc.3711

Hoerling MP, Kumar A, Zhong M (1997) El Niño, La Niña, and the nonlinearity of their teleconnections. J Clim 10(8):1769–1786. https://doi.org/10.1175/1520-0442(1997)010%3C1769:ENOLNA%3E2.0.CO;2

Hu Z-Z, Kumar A, Xue Y, Jha B (2014) Why were some La Niñas followed by another La Niña? Clim Dyn 42(3–4):1029–1042. https://doi.org/10.1007/s00382-013-1917-3

Hu Z-Z, Kumar A, Huang B, Zhu J, Zhang R-H, Jin FF (2017) Asymmetric evolution of El Niño and La Niña: the recharge/discharge processes and role of the off-equatorial sea surface height anomaly. Clim Dyn 49(7–8):2737–2748. https://doi.org/10.1007/s00382-016-3498-4

Huang R, Jilong C, Gang H (2007) Characteristics and variations of the East Asian monsoon system and its impacts on climate disasters in China. Adv Atmos Sci 24(6):993–1023. https://doi.org/10.1007/s00376-007-0993-x

Kalnay E, Kanamitsu M, Kistler R, Collins W, Deaven D, Gandin L, Iredell M et al (1996) The NCEP/NCAR 40-year reanalysis project. Bull Am Meteorol Soc 77(3):437–71. https://doi.org/10.1175/1520-0477(1996)077%3C0437:TNYRP%3E2.0.CO;2

Keenlyside NS, Latif M (2007) Understanding equatorial Atlantic interannual variability. J Clim 20(1):131–142. https://doi.org/10.1175/JCLI3992.1

Keshavamurty RN (1982) Response of the atmosphere to sea surface temperature anomalies over the equatorial Pacific and the teleconnections of the Southern Oscillation. J Atmos Sci 39(6):1241–59. https://doi.org/10.1175/1520-0469(1982)039%3C1241:ROTATS%3E2.0.CO;2

Kessler WS (2002) Is ENSO a cycle or a series of events? Geophys Res Lett 29(23):40–44. https://doi.org/10.1029/2002GL015924

Kripalani RH, Kulkarni A (1997) Climatic impact of El Niño/La Niña on the Indian monsoon: a new perspective. Weather 52(2):39–46. https://doi.org/10.1002/j.1477-8696.1997.tb06267.x

Kucharski F, Joshi MK (2017) Influence of tropical South Atlantic sea-surface temperatures on the Indian summer monsoon in CMIP5 models. Q J R Meteorol Soc 143(704):1351–1363. https://doi.org/10.1002/qj.3009

Kucharski F, Bracco A, Yoo JH, Tompkins AM, Feudale L, Ruti P, Dell'Aquila A (2009) A Gill–Matsuno-type mechanism explains the tropical Atlantic influence on African and Indian monsoon rainfall. Q J R Meteorol Soc 135(640):569–579. https://doi.org/10.1002/qj.406

Kucharski F, Parvin A, Farneti R, Rodriguez-Fonseca B, Martin-Rey M, Polo I, Mohino E, Losada T, Mechoso CR (2016) The teleconnection of the tropical Atlantic to Indo-Pacific sea surface temperatures on inter-annual to centennial time scales: a review of recent findings. Atmosphere 7(2):1–20. https://doi.org/10.3390/atmos7020029

Kug J-S, An SI, Jin F-F, Kang IS (2005) Preconditions for El Niño and La Niña onsets and their relation to the Indian Ocean. Geophys Res Lett 32(5):L05706. https://doi.org/10.1029/2004GL021674

Kumar KK, Soman MK, Kumar RK (1995) Seasonal forecasting of Indian summer monsoon rainfall: a review. Weather 50(12):449–467. https://doi.org/10.1002/j.1477-8696.1995.tb06071.x

Kumar K, Rajagopalan B, Cane MA (1999) On the weakening relationship between the Indian monsoon and ENSO. Science 284(5423):2156–2159. https://doi.org/10.1126/SCIENCE.284.5423.2156

Li CY, Mu MQ (2000) Relationship between East Asian winter monsoon, warm pool situation and ENSO cycle. Chin Sci Bull 45(16):1448–1455

Li G, Xie SP (2012) Origins of tropical-wide SST biases in CMIP multi-model ensembles. Geophys Res Lett 39(22):1–5. https://doi.org/10.1029/2012GL053777

Li G, Xie SP (2014) Tropical biases in CMIP5 multimodel ensemble: the excessive equatorial Pacific cold tongue and double ITCZ problems. J Clim 27(4):1765–1780. https://doi.org/10.1175/JCLI-D-13-00337.1

Li G, Du Y, Xu H, Ren B (2015) An intermodel approach to identify the source of excessive equatorial Pacific cold tongue in CMIP5 models and uncertainty in observational datasets. J Clim 28(19):7630–7640. https://doi.org/10.1175/JCLI-D-15-0168.1

Li G, Xie SP, Du Y, Luo Y (2016) Effects of excessive equatorial cold tongue bias on the projections of tropical Pacific climate change. Part I: the warming pattern in CMIP5 multi-model ensemble. Clim Dyn 47(12):3817–3831. https://doi.org/10.1007/s00382-016-3043-5

Li G, Xie SP, He C, Chen Z (2017) Western Pacific emergent constraint lowers projected increase in Indian summer monsoon rainfall. Nat Clim Change 7(10):708–712. https://doi.org/10.1038/nclimate3387

Loon van H, Shea DJ (1985) The Southern Oscillation. Part IV: the precursors south of 15°S to the extremes of the oscillation. Mon Weather Rev 113(12):2063–2074. https://doi.org/10.1175/1520-0493(1985)113%3C2063:TSOPIT%3E2.0.CO;

Lübbecke JF, McPhaden MJ (2013) A comparative stability analysis of Atlantic and Pacific Niño modes. J Clim 26(16):5965–5980. https://doi.org/10.1175/JCLI-D-12-00758.1

Luo J-J, Liu G, Hendon H, Alves O, Yamagata T (2017) Inter-basin sources for two-year predictability of the multi-year La Niña event in 2010–2012. Sci Rep 7(1):2276. https://doi.org/10.1038/s41598-017-01479-9

Matsuno T (1966) Quasi-geostrophic motions in the equatorial area. J Meteorol Soc Jpn Ser II 44(1):25–43. https://doi.org/10.2151/jmsj1965.44.1_25

Ohba M, Ueda H (2009) Role of nonlinear atmospheric response to SST on the asymmetric transition process of ENSO. J Clim 22(1):177–192. https://doi.org/10.1175/2008JCLI2334.1

Okumura YM, Deser C (2010) Asymmetry in the duration of El Niño and La Niña. J Clim 23(21):5826–5843. https://doi.org/10.1175/2010JCLI3592.1

Okumura YM, Ohba M, Deser C, Ueda H (2011) A proposed mechanism for the asymmetric duration of El Niño and La Niña. J Clim 24(15):3822–3829. https://doi.org/10.1175/2011JCLI3999.1

Okumura YM, DiNezio P, Deser C (2017) Evolving impacts of multi-year La Niña events on atmospheric circulation and U.S. drought. Geophys Res Lett 44(22):11, 614–11, 623

Pai DS, Sridhar L, Badwaik MR, Rajeevan M (2015) Analysis of the daily rainfall events over India using a new long period (1901–2010) high resolution (0.25° × 0.25°) gridded rainfall data set. Clim Dyn 45(3–4):755–776. https://doi.org/10.1007/s00382-014-2307-1

Pant G, Parthasarathy SB (1981) Some aspects of an association between the southern oscillation and Indian summer monsoon. Arch Meteorol Geophys Bioclimatol Ser B 29:245–252

Philander SGH (1983) El Niño southern oscillation phenomena. Nature 302(5906):295–301. https://doi.org/10.1038/302295a0

Polo I, Martin-Rey M, Rodriguez-Fonseca B, Kucharski F, Mechoso CR (2014) Processes in the Pacific La Niña onset triggered by the Atlantic Niño. Clim Dyn 44(1–2):115–131. https://doi.org/10.1007/s00382-014-2354-7

Pottapinjara V, Girishkumar MS, Ravichandran M, Murtugudde R (2014) Influence of the Atlantic zonal mode on monsoon depressions in the Bay of Bengal during boreal summer. J Geophys Res Atmos 119(11):6456–6469. https://doi.org/10.1002/2014JD021494

Rajeevan M, Bhate J, Kale JD, Lal B (2006) High resolution daily gridded rainfall data for the Indian region: analysis of break and active monsoon spells. Curr Sci 91(3):296–306

Ramu DA, Sabeerali CT, Chattopadhyay R, Nagarjuna Rao D, George G, Dhakate AR, Salunke K, Srivastava A, Rao SA (2016) Indian summer monsoon rainfall simulation and prediction skill in the CFSv2 coupled model: impact of atmospheric horizontal resolution. J Geophys Res Atmos 121(5):2205–2221. https://doi.org/10.1002/2015JD024629

Ramu DA, Chowdary JS, Ramakrishna VS, Kumar OS (2018) Diversity in the representation of large-scale circulation associated with ENSO-Indian summer monsoon teleconnections in CMIP5 models. Theor Appl Climatol 132(1–2):465–478. https://doi.org/10.1007/s00704-017-2092-y

Rasmusson EM (1985) El Niño and variations in climate: large-scale interactions between the ocean and the atmosphere over the tropical Pacific can dramatically affect weather patterns around the world. Am Sci 73(2):168–177

Rayner NA, Parker DE, Horton EB, Folland CK, Alexander LV, Rowell DP, Kent EC, Kaplan A (2003) Global analyses of sea surface temperature, sea ice, and night marine air temperature since the late nineteenth century. J Geophys Res 108(D14):4407. https://doi.org/10.1029/2002JD002670

Rodríguez-Fonseca B, Polo I, García-Serrano J, Losada T, Mohino E, Mechoso CR, Kucharski F (2009) Are Atlantic Niños enhancing Pacific ENSO events in recent decades? Geophys Res Lett. https://doi.org/10.1029/2009GL040048

Sampe T, Xie SP (2010) Large-scale dynamics of the Meiyu-Baiu rainband: environmental forcing by the westerly jet. J Clim 23(1):113–134. https://doi.org/10.1175/2009JCLI3128.1

Sikka DR (1980) Some aspects of the large scale fluctuations of summer monsoon rainfall over India in relation to fluctuations in the planetary and regional scale circulation parameters. J Earth Syst Sci 89(2):179–195. https://doi.org/10.1007/BF02913749

Singh P, Chowdary JS, Gnanaseelan C (2013) Impact of prolonged La Niña events on the Indian Ocean with a special emphasis on southwest Tropical Indian Ocean SST. Glob Planet Change 100:28–37. https://doi.org/10.1016/J.GLOPLACHA.2012.10.010

Song F, Zhou T, Qian Y (2014) Responses of East Asian summer monsoon to natural and anthropogenic forcings in the 17 latest

CMIP5 models. Geophys Res Lett 41(2):596–603. https://doi.org/10.1002/2013GL058705

Takaya K, Nakamura H (2001) A formulation of a phase-independent wave-activity flux for stationary and migratory quasigeostrophic eddies on a zonally varying basic flow. J Atmos Sci 58(6):608–627. https://doi.org/10.1175/1520-0469(2001)058%3C0608:AFOAPI%3E2.0.CO;2

Taylor KE, Stouffer RJ, Meehl GA (2012) An overview of CMIP5 and the experiment design. Bull Am Meteorol Soc 93(4):485–498. https://doi.org/10.1175/BAMS-D-11-00094.1

Trenberth KE, Hoar TJ (1997) El Niño and climate change. Geophys Res Lett 24(23):3057–3060. https://doi.org/10.1029/97GL03092

Wang CZ (2002) Atmospheric circulation cells associated with the El Niño-southern oscillation. J Clim 15(4):399–419. https://doi.org/10.1175/1520-0442(2002)015%3C0399:ACCAWT%3E2.0.CO;2

Wang B, Wu R, Lau K-M (2001) Interannual variability of the Asian summer monsoon: contrasts between the Indian and the Western North Pacific–East Asian monsoons. J Clim 14(20):4073–90. https://doi.org/10.1175/1520-0442(2001)014%3C4073:IVOTAS%3E2.0.CO;2

Wang B, Wu R, Li T (2003) Atmosphere–warm ocean interaction and its impacts on Asian–Australian monsoon variation. J Clim 16(8):1195–1211. https://doi.org/10.1175/1520-0442(2003)16%3C1195:AOIAII%3E2.0.CO;2

Webster PJ, Yang S (1992) Monsoon and ENSO: selectively interactive systems. Q J R Meteorol Soc 118(507):877–926. https://doi.org/10.1002/qj.49711850705

Webster PJ, Magaña VO, Palmer TN, Shukla J, Tomas RA, Yanai M, Yasunari T (1998) Monsoons: processes, predictability, and the prospects for prediction. J Geophys Res Oceans 103(C7):14451–14510. https://doi.org/10.1029/97JC02719

Wu B, Li T, Zhou T (2010) Asymmetry of atmospheric circulation anomalies over the Western North Pacific between El Niño and La Niña. J Clim 23(18):4807–4822. https://doi.org/10.1175/2010JCLI3222.1

Yadav RK (2009a) Changes in the large-scale features associated with the Indian summer monsoon in the recent decades. Int J Climatol 29(1):117–133. https://doi.org/10.1002/joc.1698

Yadav RK (2009b) Role of equatorial central Pacific and Northwest of North Atlantic 2-metre surface temperatures in modulating Indian summer monsoon variability. Clim Dyn 32(4):549–563. https://doi.org/10.1007/s00382-008-0410-x

Yadav RK (2017) On the relationship between east equatorial Atlantic SST and ISM through Eurasian wave. Clim Dyn 48(1–2):281–295. https://doi.org/10.1007/s00382-016-3074-y

Yadav RK, Srinivas G, Chowdary JS (2018) Atlantic Niño modulation of the Indian summer monsoon through Asian jet. Clim Atmos Sci. https://doi.org/10.1038/s41612-018-0029-5

Yu JY, Mechoso CR (1999) Links between annual variations of Peruvian stratocumulus clouds and of SSTs in the eastern equatorial Pacific. J Clim 12(1993):3305–3318

Zebiak SE (1993) Air–sea interaction in the equatorial Atlantic region. J Clim. https://doi.org/10.1175/1520-0442(1993)006%3C1567:AIITEA%3E2.0.CO;2

Zheng F, Feng L, Zhu J (2015) An incursion of off-equatorial subsurface cold water and its role in triggering the 'Double Dip' La Niña event of 2011. Adv Atmos Sci 32(6):731–742. https://doi.org/10.1007/s00376-014-4080-9